2017

# Identification, Calculation and Warning of Horizontal Curves for Low-volume Two-lane Roadways Using Smartphone Sensors

Shaohu Zhang
*South Dakota State University*

# IDENTIFICATION, CALCULATION AND WARNING OF HORIZONTAL CURVES FOR LOW-VOLUME TWO-LANE ROADWAYS USING SMARTPHONE SENSORS

BY

SHAOHU ZHANG

A thesis submitted in partial fulfillment of the requirements for the

Master of Science

Major in Civil Engineering

South Dakota State University

2017

IDENTIFICATION, CALCULATION AND WARNING OF HORIZONTAL CURVES FOR LOW-VOLUME TWO-LANE ROADWAYS USING SMARTPHONE SENSORS

SHAOHU ZHANG

This thesis is approved as a creditable and independent investigation by a candidate for the Master of Science in Civil Engineering degree and is acceptable for meeting the thesis requirements for this degree. Acceptance of this thesis does not imply that the conclusions reached by the candidate are necessarily the conclusions of the major department.

Jonathan Wood, Ph.D. Date
Thesis Advisor

Nadim Wehbe, Ph.D., P.E. Date
Head, Department of Civil & Environmental Engineering

Dean, Graduate School Date

# Dedications

Dedicated to

My lovely wife and son

In honor of,

The study and life at SDSU

Code, study, think, sleep, repeat

In memory of,

My beloved grandparents

# ACKNOWLEDGEMENTS

I would like to take this opportunity to thank my thesis advisor Dr. Jonathan Wood for his excellent guidance, caring, and providing me with great support for doing this research. His ideas and insights were most valuable at critical moments of the research for this thesis. The wealth of knowledge and the method of exploring I learned from him will be a great treasure for my future research.

I would also like to thank my previous advisors or co-advisors in both Civil Engineering and Computer Science masters, Dr. Xiao Qin, Dr. Wei Wang and Dr. Myounggyu Won. Their support and assistance greatly helped me making this project moving forward. I would also like to thank all my peer students and committee members for helping me during the graduate studies.

Finally, and most importantly, I would like to express my sincere gratitude to my family members, my farther, Peisheng Zhang and my mother, Liushi Zhang. Thank them for giving me life, raising me and supporting me for studying abroad. Thank my wife Shuang. Her support, encouragement, and unwavering love have been standing beside me throughout the past six years of my life. I also would like to thank my uncle Dr. Liming Lai and my aunt Dr. Jiuhuan Feng. I could not reach so far without their support.

# TABLE OF CONTENTS


1. INTRODUCTION ........................................ 1

1.1 Motivation ........................................ 1

1.2 Objectives ........................................ 3

1.3 Contributions ........................................ 5

1.4 Structure and Organization ........................................ 5

2. LITERATURE REVIEW ........................................ 7

2.1 Introduction ........................................ 7

2.2 GIS Applications ........................................ 7

2.3 Image Processing based Approach ........................................ 9

2.4 Survey Vehicle ........................................ 9

2.5 Vehicle-to-infrastructure Communication ........................................ 10

2.6 Smartphone Applications for ITS ........................................ 12

3. SYSTEM ARCHITECTURE AND DESIGN ........................................ 14

3.1 Introduction ........................................ 14

3.2 C-Finder ........................................ 14

3.2.1 Data Collection Module ........................................ 15

3.2.2 Data Correction Module ........................................ 16

3.2.3 Curve Identification Module ........................................ 16

3.2.4 Curve Calculation Module ........................................ 16

3.2 C-Alert ........................................ 16

3.2.1 Smartphone Module ........................................ 18

3.2.2 Wireless Communication Module ........................................ 19

3.2.3 HUD Module ........................................ 19

4. METHODOLOGY ........................................ 21

4.1 Introduction ........................................ 21

4.2 Sensor Measurement Smoothing ........................................ 21

4.2.1 Butterworth Low-pass Filter ........................................ 21

4.2.2 Extended Kalman Filtering ........................................ 23

4.3 Identification of Horizontal Curves ........ 25
4.3.1 K-means ........ 25
4.3.2 Identifying Horizontal Curves ........ 26
4.4 Calculation of Horizontal Curves ........ 27
4.4.1 Chord Offset Method ........ 27
4.4.2 Superelevation Estimation ........ 29
4.5 Warning of Horizontal Curve ........ 30
5. FIELD EVALUATION ........ 34
5.1 Speed Assesment ........ 34
5.2 Curve Identification and Calculation ........ 35
5.3 Assessment of C-Alert ........ 40
6. CONCLUSIONS AND FUTURE WORK ........ 42
6.1 Conclusions ........ 42
6.2 Future Work ........ 43
REFERENCES ........ 44

## LIST OF FIGURES

Figure 2.1 Low Vertex Resolution of Roadway Alignment in the GIS Map ..................... 8

Figure 3.1 The Coordinate Systems of a Smartphone and a Vehicle ............................... 15

Figure 3.2 System Architecture of C-Finder.................................................................. 15

Figure 3.3 System Architecture of C-Alert..................................................................... 17

Figure 3.4 Actual Hardware of C-Alert. ......................................................................... 18

Figure 3.5 BLE Interface Screenshots in iPhone 4s. ....................................................... 19

Figure 3.6 Inverted Curve Arrows. .................................................................................. 20

Figure 4.1 Variation of the Angular Speed around Z Axis.............................................. 22

Figure 4.2 Variation of the Acceleration Rate on X axis................................................. 22

Figure 4.3 A Complete Picture of the Operation of the Extended Kalman Filter ............ 24

Figure 4.4 Raw GPS Locations (red) vs Smoothed GPS Locations (green) .................... 25

Figure 4.5 Cluster Assignments and Centroids............................................................... 27

Figure 4.6 Chord Offset Method for Curve Radius Measurement .................................. 29

Figure 4.7 Horizontal Curve Scenario. ............................................................................ 30

Figure 4.8 iOS Mobile Application Algorithm of Curve Warning.................................. 32

Figure 5.1 Test Site with Six Identified Horizontal Curves............................................. 34

Figure 5.2 Comparison of Vehicle Speed and Calibrated Speed..................................... 35

Figure 5.3 Comparison of Design Superelevation and Measured Superelevation ........... 39

Figure 5.4 Field Test Route of C-Alert............................................................................. 40

# ABSTRACT

IDENTIFICATION, CALCULATION AND WARNING OF HORIZONTAL CURVES FOR LOW-VOLUME TWO-LANE ROADWAYS USING SMARTPHONE SENSORS

SHAOHU ZHANG

2017

Smartphones and other portable personal devices that integrate global positioning systems, Bluetooth Low Energy, and advanced computing technologies have become more accessible due to affordable prices, product innovation, and people's desire to be connected. As more people own these devices, there are greater opportunities for data acquisition in Intelligent Transportation Systems, and for vehicle-to-infrastructure communication. Horizontal curves are a common factor in the number of observed roadway crashes. Identifying locations and geometric characteristics of the horizontal curves plays a critical role in crash prediction and prevention, and timely curve warnings save lives. However, most states in the US face a challenge to maintain detailed and high-quality roadway inventory databases for low volume rural roads due to the labor-intensive and time-consuming nature of collecting and maintaining the data.

This thesis proposes two smartphone applications C-Finder and C-Alert, to collect two-lane road horizontal curves data (including radius, superelevation, length, etc.), collect this data for transportation agencies (providing a low-cost alternative to mobile asset data collection vehicles), and for warning drivers of sharp horizontal curves, respectively. C-Finder is capable of accurately detecting horizontal curves by exploiting an unsupervised K-means machine learning technique. Butterworth low pass filtering was applied to reduce sensor noise. Extended Kalman filtering was adopted to improve GPS accuracy. Chord method-based radius computation, and superelevation estimation were introduced to achieve accurate and robust results despite of the low-frequency GPS and noisy sensor signals obtained from the smartphone. C-Alert applies BLE technology and a head-up display (HUD) to track driver speed and compare vehicle position with curve locations in a real-time fashion. Messages can be wirelessly communicated from the smartphone to a receiving unit through BLE technology, and then displayed by HUD on the vehicle's front windshield. The field test demonstrated that C-Finder achieves high curve identification accuracy, reasonable accuracy for calculating curve radius and superelevation compared to the previous road survey studies, and C-Alert indicates relatively high accuracy for speeding warning when approaching sharp curves.

# 1. INTRODUCTION

## 1.1 Motivation

Two-lane roadways are the predominant road type in most countries. There are more than 3 million two-lane highways in the United States, 90% of which carry traffic volumes less than 2,000 vehicles per day (1). According to the Fatality Analysis Reporting System (FARS) in 2014, 66.4% ( 29,796 out of 44,858) fatal crashes occurred on two-lane highways; and 20.1% (7,656 out of 38,046) of fatal crashes involved in single and two-vehicle crashes that occurred along horizontal curves (2). Therefore, knowledge of locations and geometric characteristics of the roadway curves on low-volume roads play a crucial role on crash prediction and prevention. Although some states collect and store roadway curve data, including curve-related information (i.e., curve degree) on U.S. and state highways, it is typically incomplete curve information (e.g., lacking information such as superelevation) (3). There is high demand for this information on rural roads for use in engineering design, safety management, and determining appropriate advisory speeds. This is particularly important given that the Federal Highway Administration (FHWA) has mandated that all agencies (state, local, etc.) survey all roadway horizontal curves by December 31st, 2019 (4).

All components of a smart transportation infrastructure need to be connected, monitored, and automated in order to work effectively and efficiently. Conventional one-way communication between highway infrastructure and motorists through traffic control devices (TCDs) consists of pavement markings, traffic signs, and signals cautioning drivers about changes in lane configuration, geometric characteristics, and right-of-way priority. A variety of TCDs are installed at horizontal curves to warn drivers of turning direction and reducing speed. These TCDs are typically not adapted to the driver's position and speed, it is expected that drivers notice and heed these warnings. However, the ability of a driver to see a TCD can be compromised by inclement weather, low light conditions, and vandalized or missing signs.

Horizontal curve-related crashes occur at an alarming rate. Thus, they are recognized as one of the top safety improvement focus areas by many state Departments of Transportation (DOTs). Many of these crashes can be attributed to human errors such as inattentiveness, recklessness, distraction, and driving under the influence. Human errors, however, can potentially be avoided if drivers receive advanced warnings. Active and effective communication between vehicle operators and roadway infrastructure may help to mitigate collisions.

Mobile asset data collection vehicles equipped with sensors such as LiDAR, GPS and the inertial measurement unit (IMU) can provide transportation agencies with location information and roadway design elements, including horizontal curve properties. However, users are required to be familiarized with detailed and tedious device procedures, and post-data collection processes. In addition, the cost of a survey vehicle with equipment can be prohibitive for many agencies and researchers.

As an emerging wireless technology, Bluetooth Low Energy (i.e. Bluetooth LE or BLE) gives a high performance regarding low power consumption and data throughput (4). The widespread use of BLE in mobile phones, laptops, automobiles, etc., has fueled novel applications in areas such as healthcare, fitness, security, home automation industries and intelligent transportation systems (ITS) (4-9). Smartphones with BLE technology are an ideal choice for vehicle-to-infrastructure (V2I) communications. Smartphones that integrate GPS, IMU, BLE and advanced computing technologies have become more accessible due to affordable price, product innovation, and people's desire to be connected. As more people own these devices, greater opportunities arise for data acquisition in Intelligent Transportation Systems (ITS) and for vehicle-to-infrastructure (V2I) communications, leading to low-cost and real-time mobile sensor platforms.

**1.2 Objectives**

The goal of this study is to provide an off-the-shelf smartphone based application to collect horizontal curve data in a low-cost manner and prevent crashes by providing drivers with timely information about road hazards, including sharp curves. The objectives are to design, test, and evaluate smartphone technologies and wireless communications for acquiring, processing, and analyzing sensor data and providing users with curve information. The main steps required to meet these objectives include:

- Defining the system architecture and functional requirements, and
- Evaluating the system reliability and integration

These steps are described in further detail below.

1) *Define the System Architecture and Functional Requirements*

Smartphones have relatively low cost sensors chips. The low cost is associated with a reduction in accuracy, compared to more expensive sensors. Thus, when using these sensors, it is critical to improve the sensors' accuracy. This requires a system that 1) accounts for and reduces sensor (e.g., gyro and accelerometer) measurement errors and outliers; 2) reduces the location error caused by the weak GPS signals or GPS outage; and 3) provides a cost-effective real-time mobile system that detects horizontal curves and calculates their parameters accurately and reliably (e.g., radius and superelevation).

The concept of providing drivers with direct warning of an approaching hazard is straightforward. However, its implementation requires a system that 1) minimizes in-vehicle distractions to drivers; 2) provides timely, meaningful, and dependable messages; and 3) sustains reliable communication between the HUD and message generator (e.g., smartphone application). The key to the success requires the acquisition, delivery, and analysis of GPS data.

2) *Evaluate System Reliability and Integration*

Calculating accurate curve parameters is needed to account for sensor (e.g. gyro and accelerometer) measurement errors and outliers. Some filtering approaches (e.g. Butterworth filter and Kalman filter) can be adopted to reduce signal errors. Machine learning technique is applied to identify curves.

In order for drivers to heed warnings from V2I communications, the system must be reliable. Reliable vehicle to roadside communication is dependent on the integration of multiple systems: GPS tracks vehicle path and measures the distance to the next point of interest; smartphone application stores location-specific information of curves and processes GPS signals; wireless communication transmits real-time message to the HUD; and the HUD projects clear and concise message to vehicle’s windshields. Matching technologies to functional requirements are an important consideration.

## 1.3 Contributions

1) This study proposed an automated low-cost mobile road inventory system (C-Finder) for two-lane horizontal curve based on off-the-shelf smartphones. The proposed system is capable of accurately detecting horizontal curves by smartphone sensor data. This is accomplished by applying an extended Kalman filtering approach and a K-means machine learning technique to the data.

2) This thesis evaluated the radius and superelevation of curves using the low-cost smartphone. The experiment illustrated that the proposed approach has a relatively high accuracy. This provides a low-cost alternative to commercial data collection systems for obtaining the parameters of horizontal curves by the transportation agencies and researchers.

3) This study also developed a prototype smartphone application (C-Alert) that tracks driver position, computes arrival time at an imminent hazard (e.g., sharp curve), and alerts drivers through HUD technology. The application may improve driver decision making. It may also reduce the need for the state departments of transportation to retrofit curves.

## 1.4 Structure and Organization

The rest of this thesis is organized into five sections. Section 2 starts with the review of previous research, including the tools and approaches to collect horizontal curves, V2I communication, and smartphone applications in ITS. Advantages and disadvantages of each method are discussed.

Section 3 demonstrates the system architecture and design of C-Finder and C-Alert, respectively. C-Finder consists of four modules including Data Collection, Data Correction, Curve Identification, and Curve Calculation. C-Alert is comprised of three modules including smartphone module, communication module, and HUD module. Each module is specified addressed.

Section 4 provides the methodology to filtering sensor data, identifying curves and calculating curves. Butterworth low filtering is used to reduce the sensor errors. K-means machine learning technique is adopted to identify horizontal curves. Chord offset method is applied to calculate the averaged radius of curves. The proposed superelevation estimation approach is introduced. The approach of warning sharp horizontal curves is addressed.

Section 5 provides the field evaluation. The speed obtained from the smartphone and the identification accuracy of curves are assessed. Then, the radius and superelevation modules are evaluated. Finally, the curve warning of C-Alert is evaluated.

Section 6 presents the summary, conclusions and recommended future work based on this study

# 2. LITERATURE REVIEW

## 2.1 Introduction

Many agencies and researchers have shown interests in the extraction and identification of horizontal curves since they are considered as hazardous roadway locations. Common curve identification techniques employed involve geographic information systems (GIS) based tools, satellite imagery processing, and the mobile asset data collection. This literature review includes the definitions, procedures, methodologies, and applications of identification, calculation and warning of horizontal curves used in previous studies.

## 2.2 GIS Applications

Three main GIS-based methods are used in the published literature: Curve Calculator (ArcGIS), Curvature Extension (*5*) and Curve Finder (*6*). Curve Calculator was developed by the Environmental Systems Research Institute (ESRI). It allows users to manually define the beginning and ending of a curve and input any two of four curve characteristics (i.e., chord length, angle, arc length, and radius) to each curve. This is accomplished by inputting the information for a single curve at a time. Curvature Extension was developed by the Florida Department of Transportation (FDOT). Similar to Curve Calculator, users must manually define the beginning and ending of a curve and input parameters of the curve for the individual curves. Curve Finder is a program developed by the New Hampshire Department of Transportation (NHDOT), which allows for an automated procedure that can be executed on a network of roadways. Curves are identified as the program moves through a series of points.in a GIS polylines file.

GIS-based tools (*3; 7; 8*) can extract and identify horizontal curves from GIS roadway maps in  large-scale networks. Recently Li et al. demonstrated that Curve Finder can be applied to low-volume rural roads from a selected roadway layer for classifying curves, computing curve geometries and creating a geographic information system for curve layers automatically (*3*). Li et al. showed that GIS tools provide an inexpensive and efficient way to obtain curve information. However, the GIS-based techniques require high-quality GIS data to reduce the identification errors from transverse measurement errors and low vertex resolution of the GIS roadway centerline as shown in Figure 2.1. In addition, it is not possible to evaluate the superelevation of horizontal curves based on GIS data and tools.

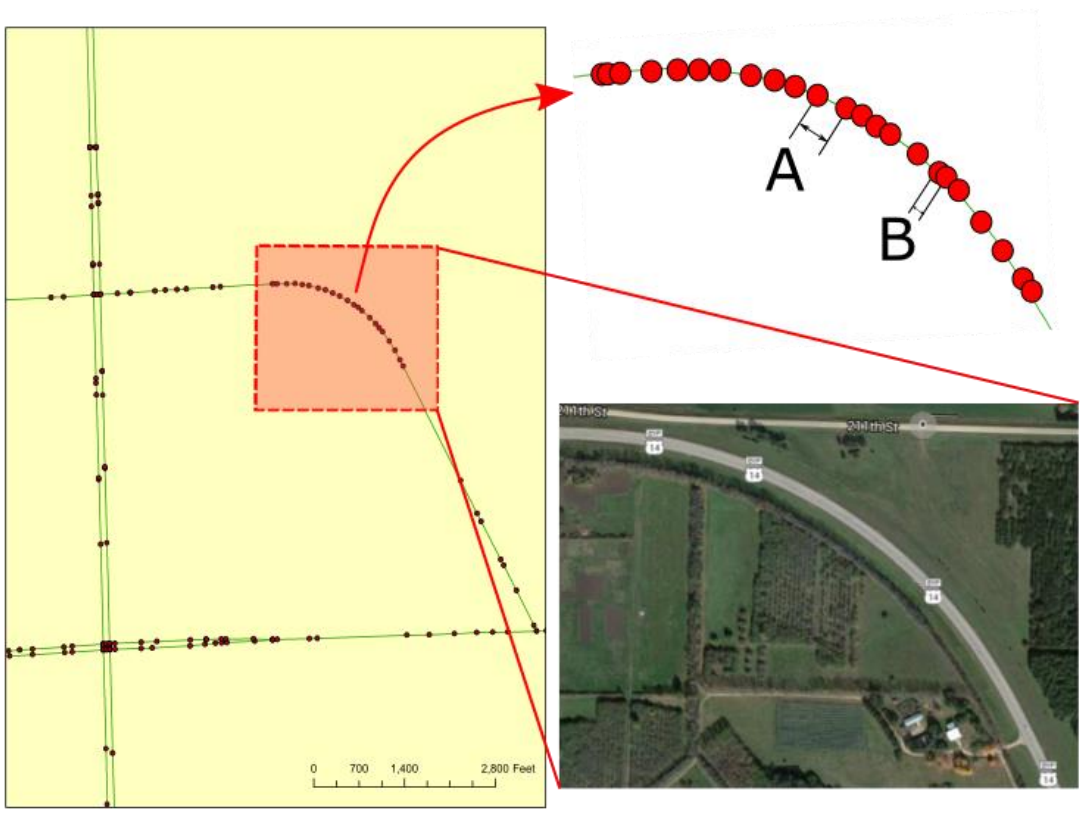


**Figure 2.1 Low Vertex Resolution of Roadway Alignment in the GIS Map**

## 2.3 Image Processing based Approach

Image processing using high-resolution satellite imagery (*9-12*) can retrieve geometric characteristics of some typical curves. For instance, Easa et al. designed a method using IKONOS 1m spatial resolution imagery to extract simple circular and reversed curve information (*13*). Dong et al. applied the Hough Transform algorithm to develop an approximate method for extracting spiral horizontal curves using high-resolution satellite imagery (*14*). Although these approaches can retrieve geometric characteristics of some typical curves by using an approximation algorithm, the limitations are that the accuracy relies on image resolution and that it requires processing of a large number of high-resolution images. Thus, these methods incur high computational costs. Also, none of these methods can extract information of the superelevation of the horizontal curves.

## 2.4 Survey Vehicle

A survey vehicle equipped with a GPS receiver, inertial system and other sensors (e.g., LiDAR) is a common way to collect data and construct roadway asset inventories. The collected raw GPS data are post-processed to extract horizontal curve components. Harkey et al. (*15*) discussed how the azimuth data obtained from the automated vehicle can be a useful tool for identifying curves and tangents on the roadway. However, the data collection and the post-processing methods need to be improved to measure the radius and length of horizontal curves accurately. Carlson et al. (*16*) identified and tested ten techniques (i.e. basic ball bank indicator (BBI), advanced BBI, chord length, compass, field survey, GPS, lateral acceleration, plan sheet, speed advisory plate, and vehicle yaw rate ) to obtain horizontal curve radii. Base on the results, in-vehicle GPS method was recommended to record roadway alignment for field personnel. To evaluate the accuracy of horizontal alignment data from multiple commercial roadway inventories, Findley et al. (*17*) applied five different techniques (i.e., chord method, GIS method, vendor data, survey data, and design data) to obtain curve parameters. The results were compared with the vendors' data, and the authors argued that agencies should consider the limitations of each technique to get appropriate data to meet their needs. Laser scanning technology (*18*) can provide highly accurate survey data, which can be utilized to extract the horizontal and vertical alignment of a curve. However, its cost is higher than that of other approaches, e.g., it was reported that the cost per mile to obtain the required highway inventory dataset for photo/video log, satellite/aerial imagery, and GPS data logger were $72, $107, and $700, respectively, while the mobile LiDAR was $915 (*19*). In addition, users must be familiarized with operating instructions. Finally, the post-processing of raw data from these systems is time consuming and labor intensive.

### 2.5 Vehicle-to-infrastructure Communication

The goals of improving safety, comfort, and efficiency of roadway systems motivate further development of wireless communications in ITS. The U.S. Department of Transportation (USDOT) has promoted the development of Wireless Access in Vehicular Environments (WAVE) based on IEEE 802.11p and IEEE 1609.x. A WAVE system consists of two classes of devices that allow bidirectional vehicle-to-vehicle (V2V) or vehicle-to-infrastructure (V2I) communication: roadside units (RSUs) and onboard units (OBUs) (*20*). V2I communications are an emerging technology based on wireless network protocol. Vehicles equipped with intelligent systems such as collision warning systems (CWS) or lane-keeping assistance systems (LKAS) are designed for safety (*21*).

To date, some V2I systems have been developed based on available wireless communication options such as Worldwide Interoperability for Microwave Access (WiMAX, IEEE 802.16), Wireless Fidelity (Wi-Fi, IEEE 802.11), and Dedicated Short-Range Communication (DSRC, IEEE 802.11p ) (*22*). These wireless communication technologies have been designed for traffic data acquisition and dissemination systems, work zones, intersection collision warning systems, and incident detection (*23*-*26*). Designing ITS networks balance the goals of functionality, performance, reliability and cost. However, given the limits of communication infrastructure in rural areas, the selection of suitable V2I communication alternatives can be challenging.

Typical V2I data are processed in the short-range distance with wireless communication systems. BT (Bluetooth) technology standardized as IEEE 802.15 is widely used in both industrial and commercial environments. BLE (Bluetooth Low Energy) is a new wireless technology developed by the Bluetooth Special Interest Group (SIG) for short-range communications, which use the low energy feature of the BT v4.0 specification for controlling and monitoring applications. A BLE product can collect data and run for months or years on a tiny battery (*27; 28*). Given the widespread use of BT technology, it is likely that BLE will be widely used in smartphones in the near future (*29*).

Drivers are constantly receiving information collected through in-vehicle sensors. The communication of this information could become a distraction if not presented and managed properly. Alerting drivers without creating an extra distraction is important for the driver's safety. HUD projects information on the front vehicle windshield without requiring the driver to take her/his eyes off the roadway. Due to its safe design, HUD has been gradually adopted in new vehicle models by manufacturers such as GM and BMW. Many HUD systems (*30*-*32*) and several smartphone applications (*33; 34*) have been designed or developed in recent years, and these driver-assistance devices provide navigation information such as current vehicle position, speed, traffic sign, lane configuration, etc. However, these commercially available HUD technologies are proprietary.

### 2.6 Smartphone Applications for ITS

Most smartphones are equipped with a series of sensors including an accelerometer, gyroscope, light, magnetic sensor, BLE and GPS. This richness in sensors enable support for roadway inventory in a low-cost manner. Recently, many studies have been prompted using smartphone sensing in vehicles. GPS related applications are applied to positioning capturing (*35; 36*) or to vehicle tracking (*37*). Accelerometers have been used in studies to measure potholes (*38; 39*) or pavement roughness (*40; 41*). Zhang et al. (*42*) presented a mobile system to detect horizontal curves by synthesizing smartphone sensor data and generate curve models by applying a support vector machines (SVMs) learning technique.

Smartphones powered by BLE technologies are attracting more and more attention from transportation researchers and wireless service providers due to the traffic and travel information they can provide. Manzoni et al. (*43*) used smartphone and BT technologies to present an interaction system using a V2V, as well as a driver-to-infrastructure communication system to improve motorcycle safety. The system interacts with drivers through an audio system and is remotely maintained and monitored through a web server and HTTP communications. Rodrigues et al. proposed a system architecture designed for connected vehicles using sensor-embedded smartphones, BT, a GPS receiver and accelerometer to collect and process data in real-time (*44*). Similar smartphone system architecture can also be found for V2V and V2I applications (*45*).

# 3. SYSTEM ARCHITECTURE AND DESIGN

## 3.1 Introduction

This section details the system architecture and design of C-Finder and C-Alert, respectively. C-Finder consists four modules including:

1) Data Collection,
2) Data Correction,
3) Curve Identification, and
4) Curve Calculation.

C-Alert is comprised of three modules including:

1) Smartphone module,
2) Communication module, and
3) HUD module.

Each module is specified addressed in this chapter.

## 3.2 C-Finder

The basic idea of C-Finder is to use the rotation rate around z-axis of the gyroscope to identify a curved road when a vehicle negotiates a curve. The corrected GPS location can be applied to identify the PC (point of curvature) and PT (point of tangent) of a curve, which can then be used to calculate the curve radius. Figure 3.1 illustrates the coordinate relationship between the vehicle and smartphone. As shown in Figure 3.2, The system has four main system modules: Data Collection, Data Correction, Curve Identification and Curve Calculation.

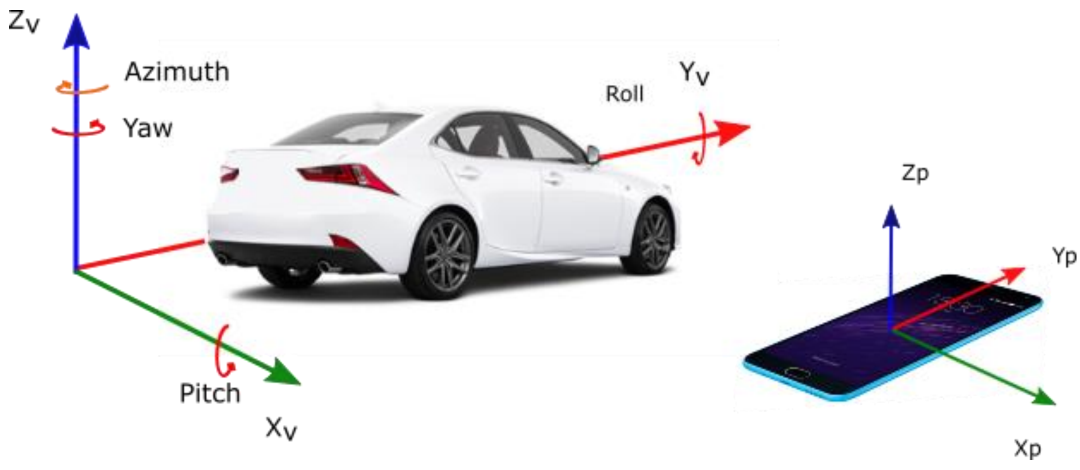


**Figure 3.1 The Coordinate Systems of a Smartphone and a Vehicle**

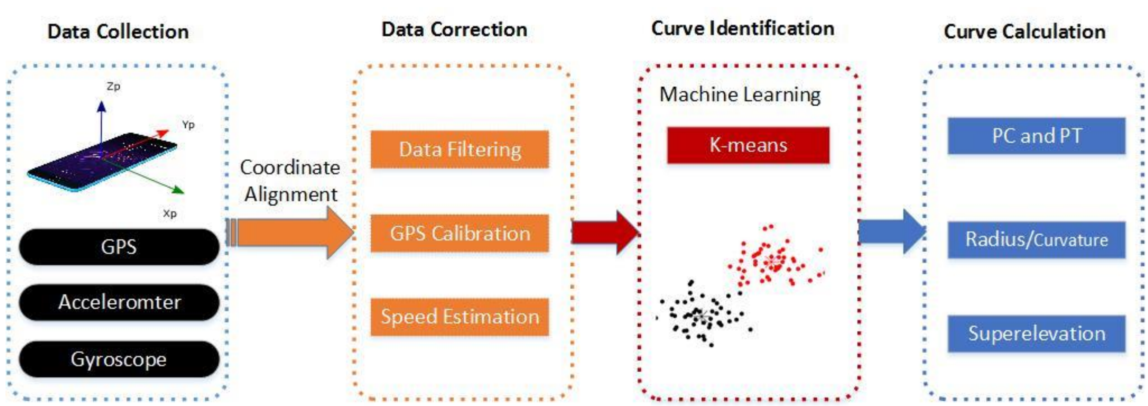


**Figure 3.2 System Architecture of C-Finder**

### *3.2.1 Data Collection Module*

This module takes as input real time sensor readings from a smartphone including the timestamp, GPS, accelerometer and gyroscope readings. GPS tracks the vehicle's position and speed. The accelerometer is to obtain the acceleration rate on the lateral direction ($X$ axis), the longitudinal direction ($Y$ axis), and the vertical direction ($Z$ axis). Gyroscope readings record the rotation rate around the lateral direction ($X$ axis), the longitudinal direction ($Y$ axis), and the vertical direction ($Z$ axis).

#### *3.2.2 Data Correction Module*

Data Correction Module reduces the noise of the raw input data. The Butterworth low filter is applied to smooth the acceleration rate ($m/s^2$) and rotation rate (rad/s). GPS and speed data are corrected by applying the extended Kalman filter (EKF) algorithm. The curved road segments can be easily detected based on the smoothed rotation rate around $Z$ axis.

#### *3.2.3 Curve Identification Module*

Once the filtered curved segment data is identified, the Curve Identification module implements the K-means machine learning algorithm to evaluate the segment data and then determine if it is the horizontal curve or not.

#### *3.2.4 Curve Calculation Module*

The obtained sensor data on the curves is imported to Curve Calculation Module. The filtered GPS data is used to identify the PC and PT of a curve, and then calculate the radius. Super elevation is calculated along with the obtained radius, speed and acceleration rate in the lateral direction.

### 3.2 C-Alert

C-Alert is comprised of three modules: smartphone module, communication module and HUD module (see Figure 3.3). Together, the three modules can track driver position, compute arrival time at an imminent hazardous location, and send alerts through HUD. In Figure 3.4, the necessary hardware includes a smartphone (iOS), a BLE shield, an Arduino, an LED matrix, and accessories (e.g., power source and cables). The work flow is designed as follows: the smartphone application sends a command to the BLE shield, then the BLE shield converts the command into digital signals and forwards them to the Arduino UNO motherboard (i.e. an embedded microprocessor). Controlled by Arduino, the LED matrix displays messages through properly connected electronic wires and pins. Eventually, the LED matrix projects a message on the windshield. A cigarette power inverter with a USB converts 12 volts of vehicle power to an alternating current (AC) for the entire system.

The rest of this section presents the detailed design and functions of each module.

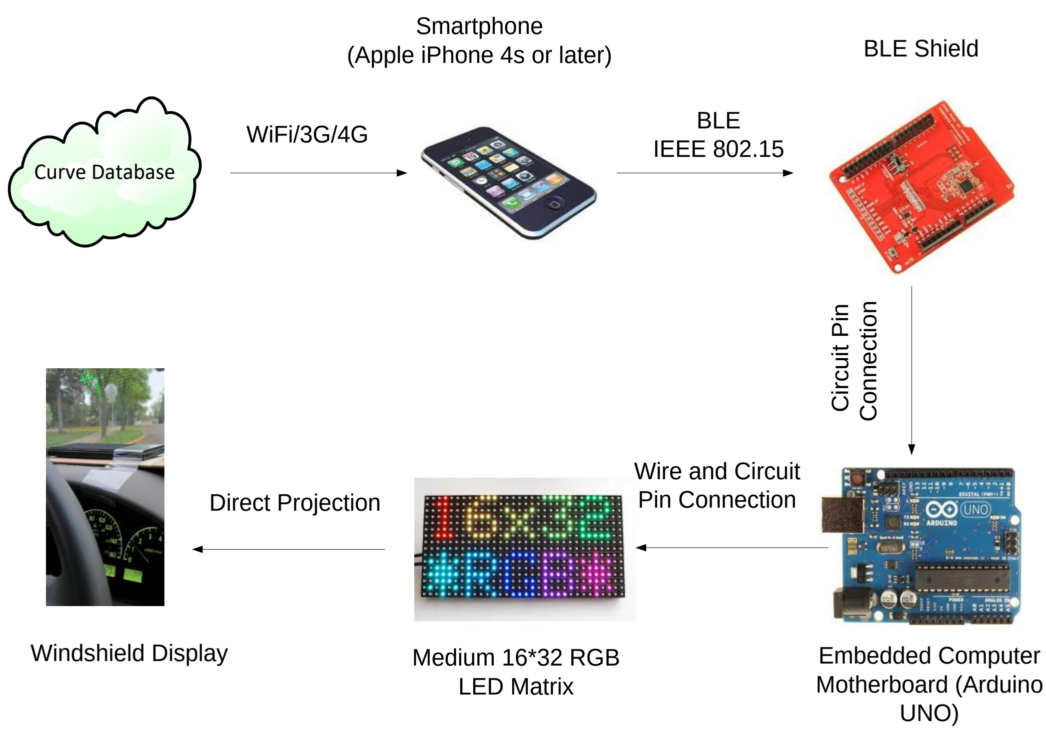


**Figure 3.3 System Architecture of C-Alert**

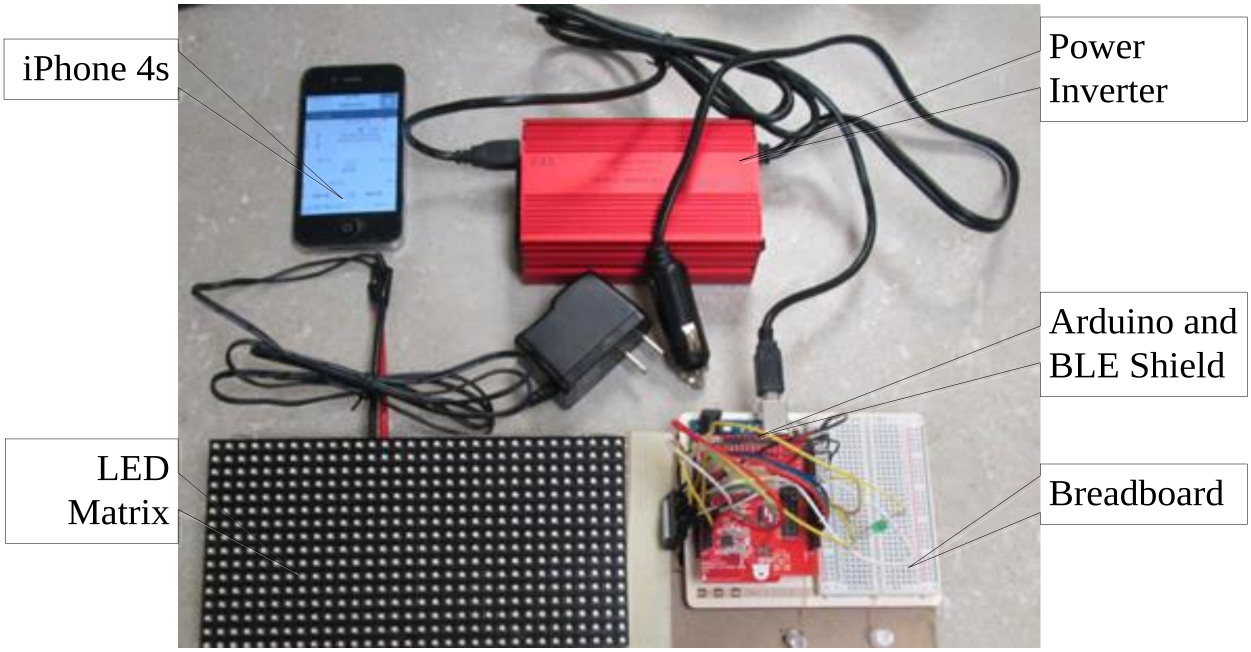


**Figure 3.4 Actual Hardware of C-Alert.**

### *3.2.1 Smartphone Module*

This module is concerned with the communication that takes place between the smartphone and the Arduino. The smartphone is the core of the system because it integrates the GPS, compass, digital map databases, and BLE communication interface. The GPS and compass provide vehicle location and orientation updates. The BLE interface allows the smartphone application to scan, connect, and communicate with the BLE through a universally unique identifier (UUID) (see Figure 3.5). Horizontal curve information (e.g., GPS coordinates, geometry, and description) can be stored in a spatial database that uses Google Maps or Apple iOS Maps as a navigational reference. For the convenience of operation, a mobile application based on Apple iPhone Operating System 7 (iOS 7) was developed using the Xcode Version 5.0 Software Development Kit (SDK) for the iPhone 4s or later models.

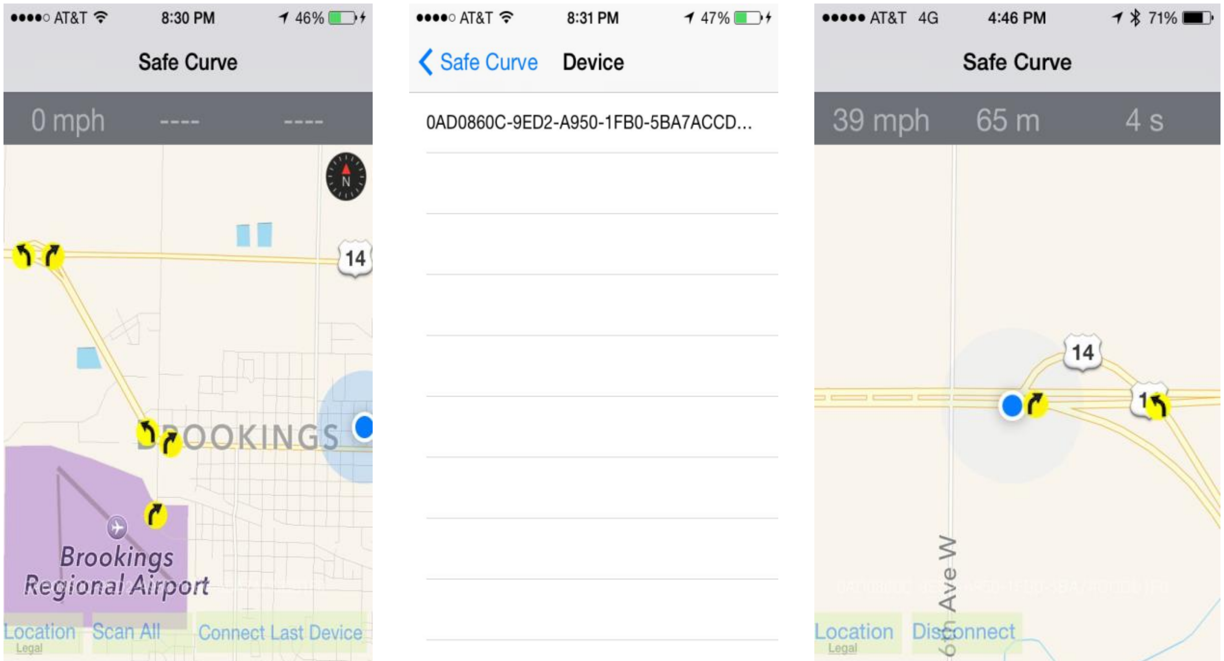


**Figure 3.5 BLE Interface Screenshots in iPhone 4s.**

### *3.2.2 Wireless Communication Module*

The Wireless communication module consists of the Arduino and BLE board. Arduino (*40*) is an open-source electronics prototyping platform. The Arduino Uno, a microcontroller board based on the ATmega328, can control physical objects. Arduino codes were developed using Arduino IDE to receive data from the BLE and send operations to control whether LED lights are on or off.

Arduino Uno does not have built-in IEEE 802.15 connectivity; thus, the BLE is added to connect and configure commands from the smartphone. BLE shield version 2 from RedBear product (*46*) was used in this research which is designed to work with the Ardunio board. The BLE shield connects to Arduino via a serial port that provides IEEE 802.15 network connectivity.

### *3.2.3 HUD Module*

**Figure 3.6 Inverted Curve Arrows.**

For the preliminary HUD, a 16×32 RGB color LED matrix panel (*47*) was used. This product has the capacity to show a variety of colors and provides a library with open source codes and a wiring tutorial (*48*) for developers. Once the display command is received by the BLE shield and the Arduino board, a program written for Arduino will control the message by sending electronic signals to the LED matrix. As illustrated in Figure 3.6, the LED matrix has such a strong light emitting intensity that the image can be clearly projected onto the windshield. Additionally, to display normal curve images, this module implements a mirroring function in the Arduino Uno program. Figure 3.6 depicts several curve images.

# 4. METHODOLOGY

## 4.1 Introduction

This chapter discusses the approaches to smoothing the noise sensor measurement. Butterworth low-pass filtering and extended Kalman filtering are introduced. A K-means machine learning technique is adopted to identify the horizontal curves. Then the radius calculation method based on a chord offset approach is describled and illustrated. The following superelevation estimation approach provides the equations this study applies. Finally, the principal method of waring horizontal curves is introduced.

## 4.2 Sensor Measurement Smoothing

### *4.2.1 Butterworth Low-pass Filter*

It is crucial to minimize measurement noise and outliers to achieve accurate curve detection and speed estimation. The Butterworth low-pass filter is well known for its effectiveness to reduce noise of high frequency measurements. This technique is adopted to remove the noise of raw accelerometer and gyroscope data collected using a smartphone. Figure 4.1 and Figure 4.2 plot measurements of rotation rate around the Z axis and acceleration rate on the X axis for a turning and a roadway curve, respectively. It is shown that the noise is effectively removed by applying the Butterworth low-pass filter.

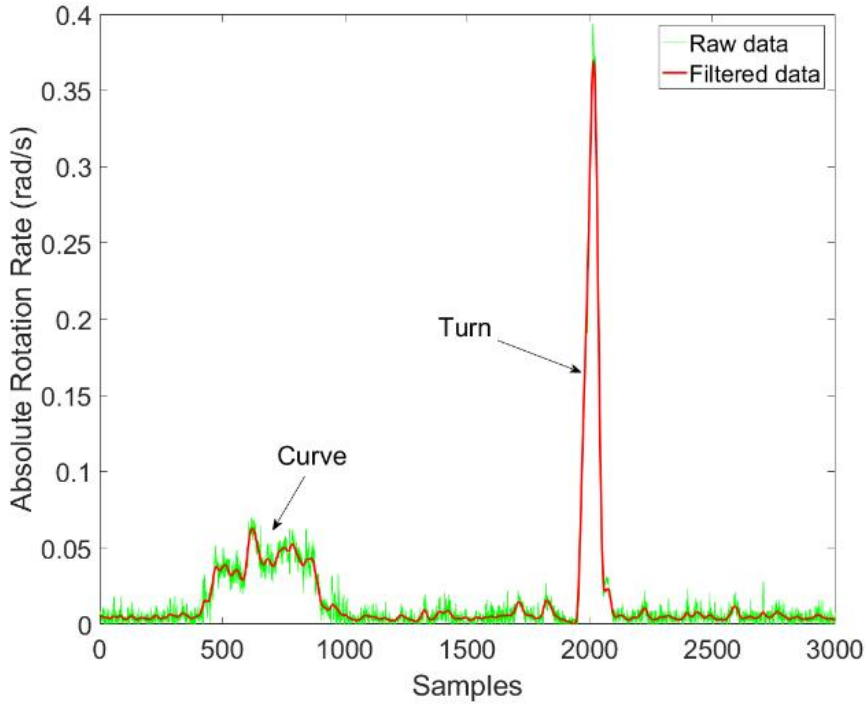


**Figure 4.1 Variation of the Angular Speed around Z Axis**

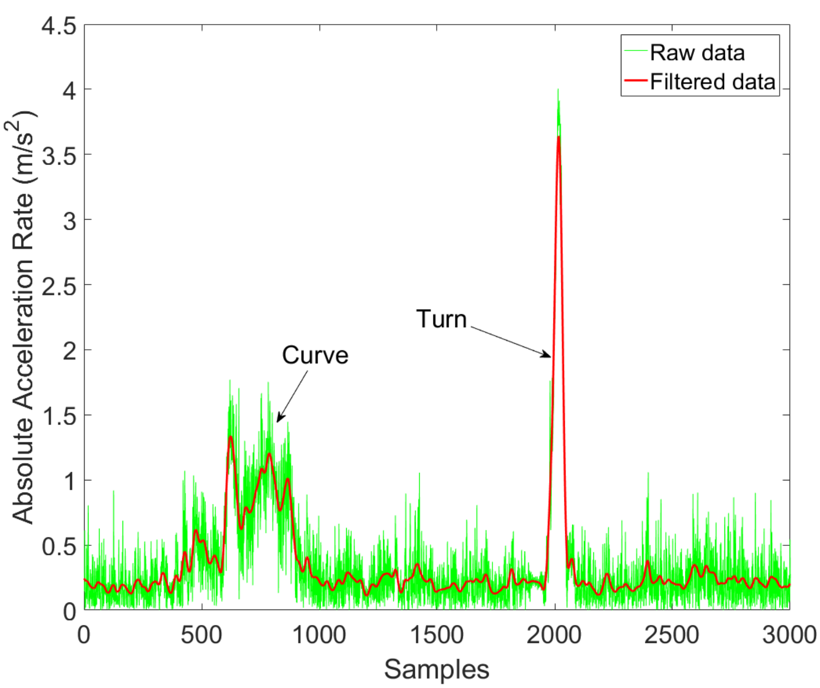


**Figure 4.2 Variation of the Acceleration Rate on X axis**

### *4.2.2 Extended Kalman Filtering*

This system requires accurate measurement of the vehicle's GPS location and speed to derive the horizontal superelevation. The smartphone can acquire the speed reading from the embedded GPS module when the GPS signal is strong. Whereas the acceleration rate and rotation rate from IMU readings can be used to calibrate vehicle's speed and locations when the GPS signal is weak or there is a signal outage.

The extended Kalman filter (EKF) is the nonlinear version of the Kalman filter which linearizes an estimate of the current mean and covariance. The EKF has been considered the de facto standard in the theory of nonlinear state estimation, navigation systems, and GPS. Assuming the process has a state vector $x_k$, and letting $f(.)$ denote the non-linear function in process. The recursion equations for EKF are given as follows.

$$x_k = f( x_{k-1}, u_{k-1}, w_{k-1}) \quad (1)$$

$$z_k = h( x_k, v_k) \quad (2)$$

where $u_{k-1}$ is the control vector; $w_{k-1}$and $v_k$ represent the process and measurement noises which are both assumed to be zero mean multivariate Gaussian noises with covariance $Q_k$ and $R_k$, respectively. The non-linear function $h()$ relates to the state $x_k$ to the measurement $z_k$.

A complete picture of the operation of the EKF is shown in Figure 4.3.

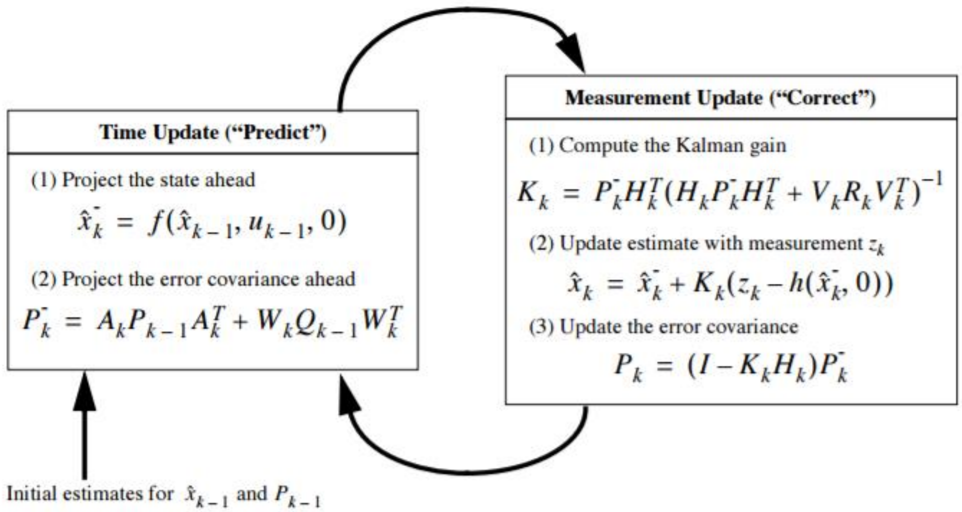


**Figure 4.3 A Complete Picture of the Operation of the Extended Kalman Filter**

(* Welch,1995(*49*))

where $A_k$ , $W_k$ , $H_k$ and $V_k$are Jacobian Matrix. The state vector x is given in equation 3.

$$x = \{lat, lon, att, v_x, v_y, v_z, w_x, w_y, w_z, acc_x, acc_y, acc_z\} \quad (3)$$

where $v$ is the speed, $w$ is the rotation rate and $acc$ is the acceleration rate. When the GPS signal is weak or outage, the speed can be evaluated by the acceleration rate, and the GPS can be estimated by rotation rate and the speed. Figure 4.4 demonstrates that the GPS accuracy is improved by using EKF.

**Figure 4.4 Raw GPS Locations (red) vs Smoothed GPS Locations (green)**

## 4.3 Identification of Horizontal Curves

### *4.3.1 K-means*

K-means is one of the common "clustering" unsupervised machine learning techniques. It partitions $n$ observations into $k$ clusters in which each observation belongs to the cluster with the nearest mean. Suppose a data set $D$, contains $n$ objects in Euclidean space, which can be partitioned into k clusters. A centroid-based partitioning technique uses the centroid of a cluster, $C_i$, to represent the $ith$ cluster. The centroid can be determined by the mean of the clusters.

The Euclidean distance, $dis(p, c_i)$, measures the distance between the object point $p$ and the centroid $c_i$. The sum of squared error (SSE) between all objects in $C_i$ is used to determine the centroid of cluster $C_i$, which can be defined as

$$SSE = \sum_{i=1}^{k} \sum_{p \in C_i} dis(p, c_i)^2 \tag{4}$$

where $p$ represent a given object, and $c_i$ is the centroid of cluster $C_i$.

### *4.3.2 Identifying Horizontal Curves*

In order to distinguish between horizontal curves and lane change or turning maneuvers, this study adopted K-means machine learning technique. With K-means clustering, a threshold is selected to remove the data from the tangent road sections. It was observed that the standard deviation and mean of the rotation rate around Z-axis have a set of clustering features. Consequently, this study was able to use K-means clustering to identify horizontal curves. K-means algorithm, with K=2, is applied to partition the training dataset into 2 clusters which represent curves and turns, respectively. Specifically, a centroid-based partitioning technique (*50*) was used to obtain the centroid of a cluster $C_i$ to represent clusters. As shown in Figure 4.5, 50 curves and 50 turns were used to train the clustering centroids. In order to identify horizontal curve displacement, a threshold (0.01 rad/s) of the rotation rate was set to obtain the points in array $A$ which represent the curved section of the vehicle's position (e.g., lane change, turns and curve). The array $A$, representing a curved road, is considered if the Euclidean distance with the centroid of curve clustering $c_i$is the smallest one based on Equation 5.

$$d = dis(A, c_i) \tag{5}$$

where $d$ is the Euclidean distance between $A$ and the $ith$ centroid in terms of the mean and standard deviation of the rotation rate around the Z axis, and $A$ is an array of the filtered rotation rate around the Z-axis.

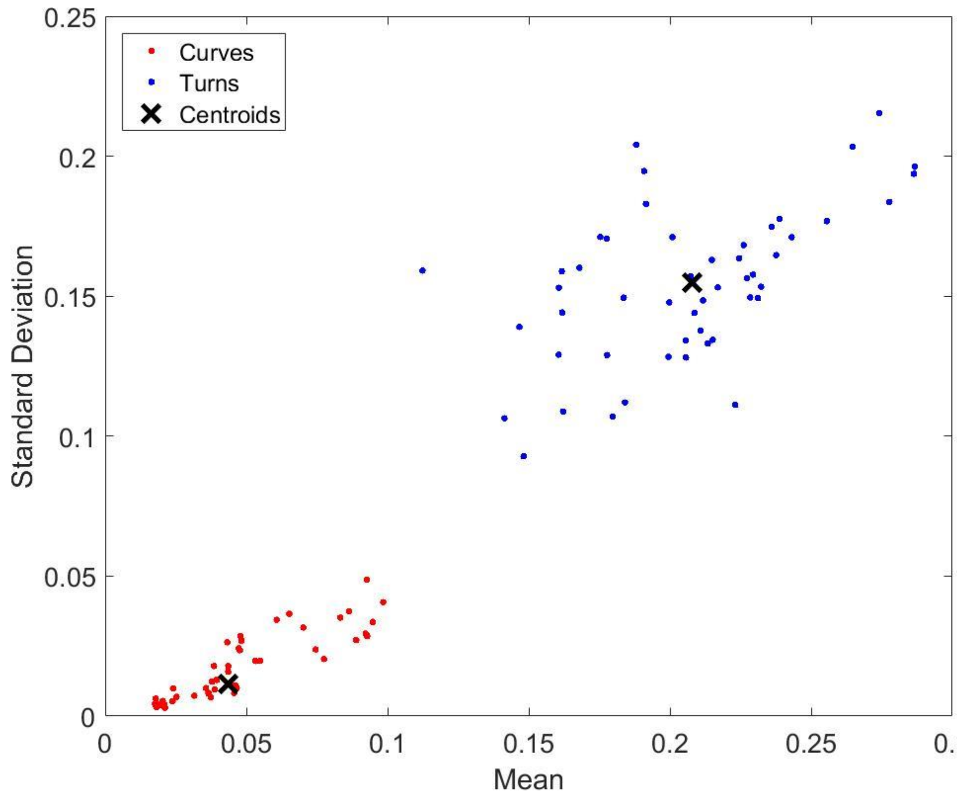


**Figure 4.5 Cluster Assignments and Centroids**

## 4.4 Calculation of Horizontal Curves

### *4.4.1 Chord Offset Method*

A chord offset method is adopted to calculate curve radius. To improve the accuracy, three measurements were recorded within the boundaries of PC and PT for each horizontal curve. In Figure 4.6**,** $R$ represents the radius of the circle in feet; $C$ is the chord length in feet; $H$ is the middle ordinate in feet. The radius in terms of $H$ and $C$ can be derived by using:

$$\frac{C^2}{4} + (R - H)^2 = R^2 \tag{6}$$

$$R = \frac{H}{2} + \frac{C^2}{8H} \pm \frac{Lane\ Width}{2} \tag{7}$$

$$D = \frac{5729.38}{R} \tag{8}$$

The GPS frequency rate is 1Hz in the majority of modern smartphones. Due to the slow rate, it cannot properly capture the locations of PC and PT of a curved road using GPS alone. The gyroscope has a much higher output rate, which can be used to identify the locations of PC and PT. More specifically, the count of samples in rotation rate over the threshold when the vehicle is traversing a curved road segment is used. This calculated proportion can be used to find the location between a point on the tangent and the next point on the curved road segment.

The chord method can be sensitive to where middle ordinate measurements are taken. To improve the accuracy of curve radius estimates, the three neighboring GPS points around the PC and PT can be used to obtain 9 chord lengths $(C)$ and 9 middle ordinate $(H)$ measurements, respectively. Equation 9 was used to calculate the chord lengths based on the observed data. Then the calculated $R_i$ was averaged using the weighted average method shown in equation 10.

$$C_i = dis(PC_j, PT_k) \tag{9}$$

$$R_{avg} = \frac{1}{9}\sum_{i=1}^{9} \frac{R_i H_i}{H_i} \tag{10}$$

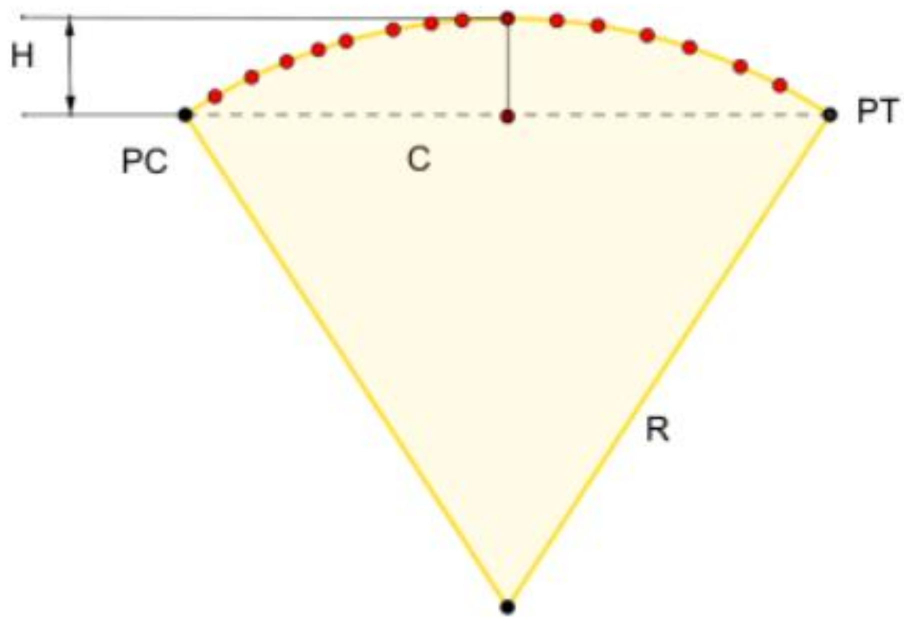


**Figure 4.6 Chord Offset Method for Curve Radius Measurement**

### *4.4.2 Superelevation Estimation*

The lateral acceleration and vehicle speed can be used to calibrate the superelevation. According to the AASHTO Green Book(*51*):

$$\frac{0.01e + f}{1 - 0.01ef} = \frac{v^2}{15R} \approx 0.01e + f \tag{11}$$

$$R = \frac{v^2}{15(0.01e + f)} \tag{12}$$

$$e = 100\left(\frac{v^2}{15R} - f\right) \tag{13}$$

where $e$ is the superelevation in percent, $f$ is the side friction factor (which is equivalent to $X_{acc}/g$), $X_{acc}$ is the acceleration rate on the side of the vehicle measured by the smartphone, and $v$ is the vehicle speed in mph;

Thus, using the calculated radius, vehicle speed, and lateral acceleration from the smartphone sensors (i.e., to obtain an estimate of $f$), the procedure of computing superelevation is straightforward.

### 4.5 Warning of Horizontal Curve

In C-Alert system, horizontal curve data are split into two types of nodes (see Figure 5): clockwise curve node and counterclockwise curve node. Their locations are relative to the coordinates of the PC (point of curvature at the beginning of curve) or the PT (point of tangency at the end of curve). PC and PT are defined on increasing mileposts.

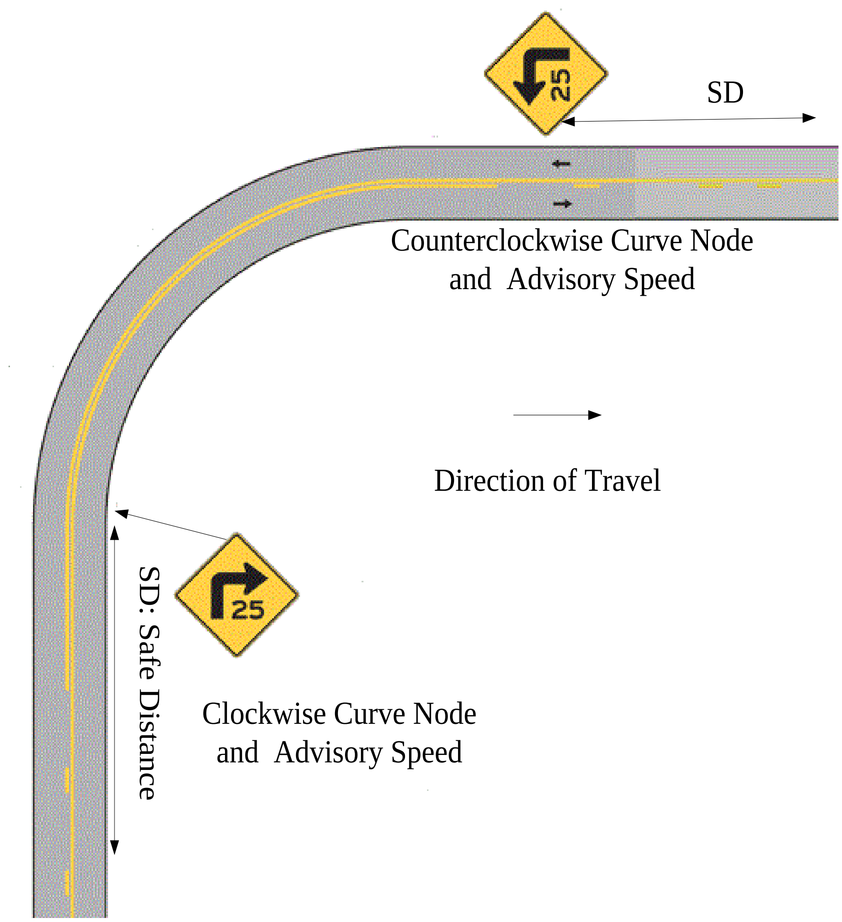


**Figure 4.7 Horizontal Curve Scenario.**

Each node is structured as shown in Equation 14.

$$\text{Node} = \{lat, lon, loc\_des, G, type, dir, v, sd\} \tag{14}$$

where $lat$ and $lon$ are the coordinates of PC or PT, *loc_des* describes a curve node including roadway name, mileage, travel direction and city or county name (e.g., a curve node located in the eastbound 421.41 miles of the highway 14 in Brookings, South Dakota, is described as "421.41 at Hwy 14 EB Brookings SD"); *G* is the roadway grade; *type* defines the horizontal curve type including simple curve, compound curve, reversed curve and spiral curve; *dir* represents the curve direction in the travel orientation; *v* is the advisory speed at the curve; and *sd* is the safe distance threshold.

Drivers can receive multiple warning messages displayed through HUD when travelling through an area with many curves; hence, it is important that messages are displayed within the proper time-frame (i.e., not too early/ not too late). Assuming a constant deceleration, the advance distance it takes a driver to perceive, react, and decelerate to the advisory speed of a curve can be calculated in equation 15, which is based on the equation of motion using Newtonian physics law.

$$S = 1.47V_0t + \frac{V_0^2 - V^2}{30\left(\frac{a}{g} \pm G\right)} \tag{15}$$

where $S$ is the minimum safe distance (feet), $V_0$ is the vehicle operating speed on a straight roadway (mph); $V$ is the advisory speed at the curve (mph); $t$ is the driver perception-reaction time (second), typically 2.5 seconds for design; $a$ is the vehicle deceleration rate (ft/s$^2$), with the recommended maximum deceleration of 0.34g used by the American Association of State Highway Transportation Officials (AASHTO); $g$ is the gravitational constant (32.2 ft/s$^2$), and $G$ is the roadway grade (+ for uphill, -for downhill) in decimal form.

An alert is activated once the vehicle enters the distance threshold for a warning. For example, a warning threshold of 15 seconds for a vehicle traveling at 60 mph is approximately 0.25 miles. Various thresholds are provided for different types of curves (e.g. a curve radius of less than 1000 feet, a hidden curve without sufficient stopping sight distance, etc.). To detect a curve within the warning distance, the built-in GPS and compass in the smartphone identify a search radius based on the safe distance and compare it with vehicle location and travel direction.

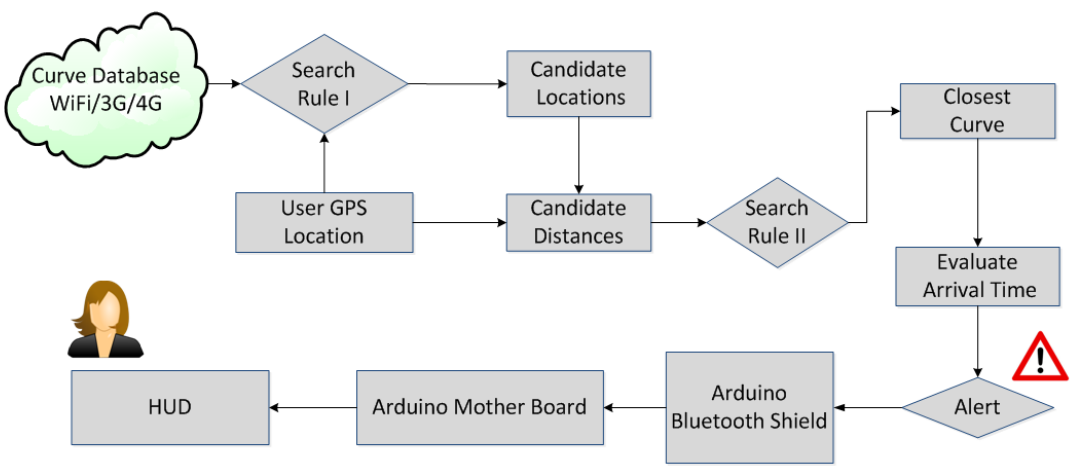


**Figure 4.8 iOS Mobile Application Algorithm of Curve Warning**

To determine the nearest curve, the smartphone module implements a two-step search algorithm as shown in Figure 4.8. Search Rule I obtains curve data from the spatial database and identifies candidate curve locations. Search Rule II identifies the nearest curve location by distance, computes travel time, sends alert commands to HUD, and displays the proper warning.

Once the vehicle enters the safe distance range, a correspondent warning is shown on the front windshield. Different signs are designed to effectively warn drivers. If the vehicle is approaching a speed below the curve's posted speed limit, HUD displays a constant green curve arrow. If the vehicle is operating at a speed within 5 mph above the posted speed limit, the system blinks a red curve arrow once per second. When the vehicle is exceeding the curve's posted speed limit by 5-10 mph, the red curve sign blinks faster at two times per second. Lastly, if the vehicle's speed is 10 mph above the posted speed limit, the red curve sign blinks at a faster rate, or four times per second. The sign disappears when vehicle has entered the curve.

# 5. FIELD EVALUATION

A Samsung Galaxy S7 Edge running Android 5 OS and an iPhone 4s running iOS 7 ware used to evaluate the system performance of C-Finder and C-Alert, respectively. The GPS frequency was collected at 1 Hz. Gyroscope and accelerometer were at 20 Hz. During these experiments, the smartphones were either mounted on the windshield, or placed in the cup holder.

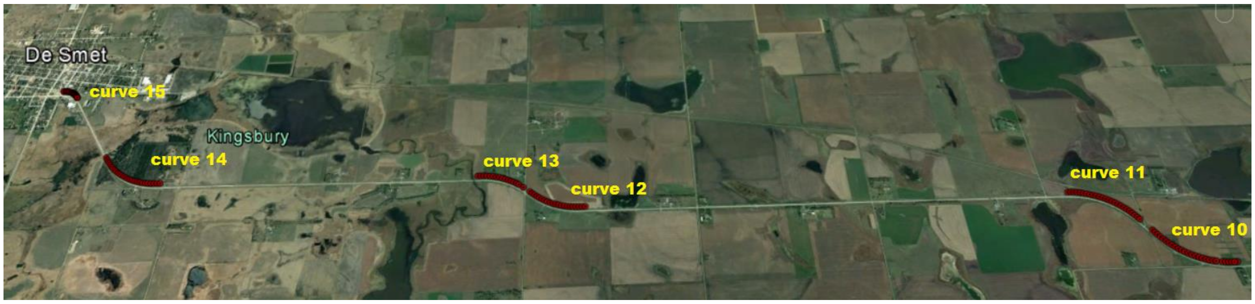


**Figure 5.1 Test Site with Six Identified Horizontal Curves**

## 5.1 Speed Assessment

Vehicle speed plays an important role in this system. In order to evaluate the speed accuracy, an On-board Diagnostics (OBD-II) sensor was applied to record the velocity from vehicle speedometer as reference. Figure 5.2 illustrates the profile of the calibrated (i.e. GPS) velocity $V_t$ and the reference (i.e. speedometer) velocity $V_r$ from OBD-II sensor.

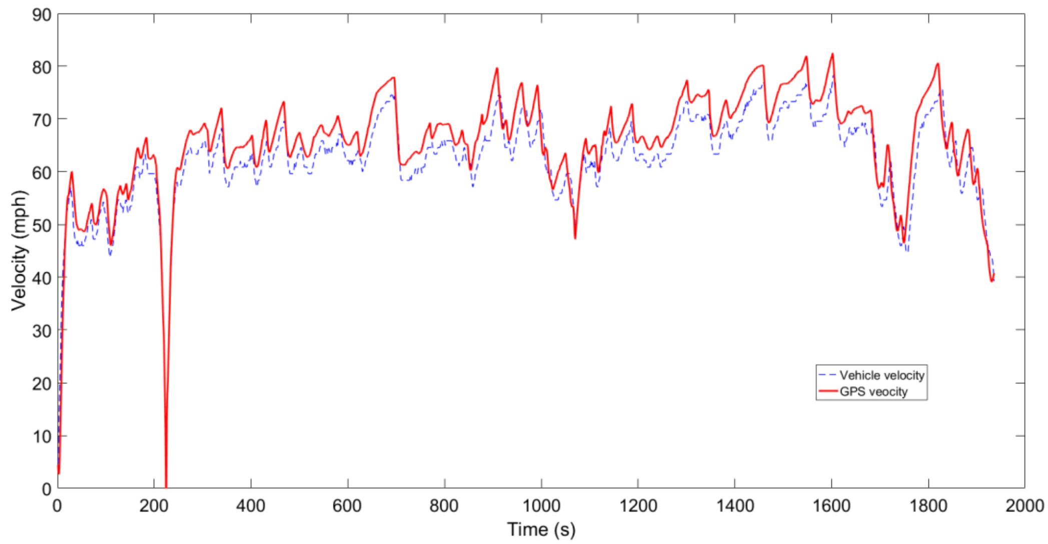


**Figure 5.2 Comparison of Vehicle Speed and Calibrated Speed**

As shown in Figure 5.2, the absolute difference between the two speed values is 0-4.5 mph with a mean value of 3.24 mph. The Mean Absolute Percentage Error (MAPE) in equation 16 was used to evaluate the speed deviation.

$$MAPE = \frac{1}{N}\sum_{n=1}^{N}\left|\frac{V_r - V_t}{V_r}\right| \tag{16}$$

where $N$ is the number of samples. The MAPE results indicated that there was approximately 6% difference between the GPS and vehicle speeds. This suggests that the speed precision obtained from smartphone is acceptable.

## 5.2 Curve Identification and Calculation

100 miles long two-lane highway located on Brookings County and Kingsbury County, South Dakota ware selected as the test area for C-Finder. This study considered the curve grade greater than 1 degree of curvature as sharp curves. A total of 21 sharp horizontal curves covering different radii were conducted. For each of these curves, roadway inventory data from SDDOT was used to compare with the estimates. All 21

horizontal curves ware identified. That means C-Finder can archive 100% accuracy to identify sharp curves in this experiment.

Three-runs surveys were measured to evaluate the stability of the proposed approach. Table 1 shows the radius measurements without adjusting for the lane width. The result indicated that the average radius difference of three runs is 3.10%, 3.44% and 3.27%, respectively. The mean radius difference is 2.2%.

**Table 1. Radius Measurement without Lane Width Adjustment**

| No | Hwy | G | Radius | Survey 1 | | Survey 2 | | Survey 3 | | Mean | |
|---|---|---|---|---|---|---|---|---|---|---|---|
| | | | | Radius | Error | Radius | Error | Radius | Error | Avg | Error |
| 1 | US13 | 5.5 | 1042 | 1180 | 13.24% | 1001 | 3.91% | 1040 | 0.19% | 1073 | 3.05% |
| 2 | US13 | 5 | 1146 | 1184 | 3.34% | 1166 | 1.76% | 1203 | 4.94% | 1184 | 3.35% |
| 3 | US13 | 1.5 | 3820 | 3601 | 5.73% | 3676 | 3.75% | 3582 | 6.21% | 3620 | 5.23% |
| 4 | US14 | 2.75 | 2083 | 2072 | 0.55% | 2050 | 1.61% | 2083 | 0.03% | 2068 | 0.73% |
| 5 | US14 | 2.5 | 2292 | 2296 | 0.18% | 2306 | 0.61% | 2291 | 0.02% | 2298 | 0.26% |
| 6 | US14 | 3 | 1910 | 1900 | 0.51% | 1943 | 1.72% | 1866 | 2.28% | 1903 | 0.36% |
| 7 | US14 | 11.25 | 509 | 455 | 10.67% | 541 | 6.19% | 544 | 6.87% | 513 | 0.80% |
| 8 | US14 | 2.5 | 2292 | 2263 | 1.26% | 2268 | 1.03% | 2280 | 0.49% | 2271 | 0.93% |
| 9 | US14 | 2.5 | 2292 | 2281 | 0.48% | 2391 | 4.34% | 2287 | 0.20% | 2320 | 1.22% |
| 10 | US14 | 2.75 | 2083 | 2083 | 0.02% | 2096 | 0.60% | 2105 | 1.06% | 2095 | 0.55% |
| 11 | US14 | 2.75 | 2083 | 2078 | 0.27% | 2046 | 1.79% | 2005 | 3.75% | 2043 | 1.94% |
| 12 | US14 | 2.75 | 2083 | 2073 | 0.50% | 2036 | 2.25% | 1956 | 6.13% | 2022 | 2.96% |
| 13 | US14 | 2.75 | 2083 | 1963 | 5.80% | 1902 | 8.71% | 1972 | 5.36% | 1945 | 6.62% |
| 14 | US14 | 2.75 | 2083 | 2108 | 1.20% | 2155 | 3.45% | 2058 | 1.22% | 2107 | 1.14% |
| 15 | US14 | 10 | 573 | 557 | 2.86% | 594 | 3.65% | 550 | 3.93% | 567 | 1.05% |
| 16 | US14B | 3 | 1910 | 1895 | 0.77% | 1961 | 2.66% | 1876 | 1.77% | 1911 | 0.04% |
| 17 | US14E | 3 | 1910 | 1904 | 0.33% | 1947 | 1.95% | 1909 | 0.07% | 1920 | 0.52% |
| 18 | US30 | 4 | 1432 | 1495 | 4.40% | 1438 | 0.40% | 1493 | 4.25% | 1476 | 3.02% |

| | | | | | | | | | | | |
|---|---|---|---|---|---|---|---|---|---|---|---|
| 19 | US30 | 5 | 1146 | 1188 | 3.71% | 1247 | 8.80% | 1214 | 5.90% | 1216 | 6.14% |
| 20 | US30 | 2 | 2865 | 2928 | 2.22% | 2961 | 3.36% | 2549 | 11.03% | 2813 | 1.82% |
| 21 | US30 | 2 | 2865 | 2663 | 7.03% | 2589 | 9.62% | 2950 | 2.97% | 2734 | 4.56% |
| **Average difference** | | | | | **3.10%** | | **3.44%** | | **3.27%** | | **2.20%** |

Table 2 shows the radius estimates with the adjustment of the lane width. The average radius difference of three runs is 2.89%, 3.06% and 3.06%, respectively. The mean radius difference is 2.06%. With the lane width adjustment, the accuracy of radius calculation is slightly improved.

**Table 2. Radius Measurement with Lane Width Adjustment**

| No | Hwy | G | Radius | Survey 1 | | Survey 2 | | Survey 3 | | Mean | |
|---|---|---|---|---|---|---|---|---|---|---|---|
| | | | | Radius | Error | Radius | Error | Radius | Error | Avg | Error |
| 1 | US13 | 5.5 | 1042 | 1173 | 12.57% | 1008 | 3.24% | 1033 | 0.86% | 1071 | 2.82% |
| 2 | US13 | 5 | 1146 | 1177 | 2.73% | 1159 | 1.15% | 1196 | 4.33% | 1177 | 2.74% |
| 3 | US13 | 1.5 | 3820 | 3594 | 5.92% | 3683 | 3.57% | 3589 | 6.03% | 3622 | 5.17% |
| 4 | US14 | 2.75 | 2083 | 2078 | 0.26% | 2056 | 1.32% | 2089 | 0.26% | 2074 | 0.44% |
| 5 | US14 | 2.5 | 2292 | 2290 | 0.08% | 2300 | 0.35% | 2297 | 0.24% | 2296 | 0.17% |
| 6 | US14 | 3 | 1910 | 1906 | 0.20% | 1937 | 1.41% | 1872 | 1.96% | 1905 | 0.25% |
| 7 | US14 | 11.25 | 509 | 461 | 9.49% | 535 | 5.01% | 538 | 5.69% | 511 | 0.41% |
| 8 | US14 | 2.5 | 2292 | 2256 | 1.56% | 2275 | 0.73% | 2273 | 0.80% | 2268 | 1.03% |
| 9 | US14 | 2.5 | 2292 | 2288 | 0.17% | 2384 | 4.03% | 2294 | 0.11% | 2322 | 1.32% |
| 10 | US14 | 2.75 | 2083 | 2091 | 0.34% | 2088 | 0.24% | 2098 | 0.70% | 2092 | 0.43% |
| 11 | US14 | 2.75 | 2083 | 2085 | 0.09% | 2054 | 1.43% | 2013 | 3.39% | 2051 | 1.58% |
| 12 | US14 | 2.75 | 2083 | 2080 | 0.14% | 2029 | 2.61% | 1963 | 5.77% | 2024 | 2.84% |
| 13 | US14 | 2.75 | 2083 | 1970 | 5.44% | 1910 | 8.35% | 1979 | 5.00% | 1953 | 6.26% |
| 14 | US14 | 2.75 | 2083 | 2116 | 1.56% | 2148 | 3.09% | 2065 | 0.86% | 2110 | 1.26% |
| 15 | US14 | 10 | 573 | 564 | 1.55% | 586 | 2.34% | 558 | 2.62% | 569 | 0.61% |
| 16 | US14B | 3 | 1910 | 1901 | 0.45% | 1955 | 2.34% | 1882 | 1.46% | 1913 | 0.14% |

| | | | | | | | | | | |
|---|---|---|---|---|---|---|---|---|---|---|
| 17 | US14E | 3 | 1910 | 1898 | 0.64% | 1953 | 2.26% | 1915 | 0.25% | 1922 | 0.62% |
| 18 | US30 | 4 | 1432 | 1489 | 3.99% | 1432 | 0.02% | 1487 | 3.83% | 1470 | 2.60% |
| 19 | US30 | 5 | 1146 | 1195 | 4.28% | 1240 | 8.23% | 1220 | 6.47% | 1218 | 6.33% |
| 20 | US30 | 2 | 2865 | 2935 | 2.45% | 2954 | 3.13% | 2555 | 10.81% | 2815 | 1.74% |
| 21 | US30 | 2 | 2865 | 2670 | 6.80% | 2596 | 9.39% | 2943 | 2.75% | 2736 | 4.48% |
| | **Average difference** | | | | **2.89%** | | **3.06%** | | **3.06%** | | **2.06%** |

This experiment indicated that drivers might reduce speed when the vehicle is approaching to a curve, which generates more sensor noise, while the vehicle status is more “smooth” when leaving out of a curve due to the reduced speed. This is consistent with previous research findings(*52-54*). For typical superelevation transitions, 90% of the transition occurs prior to the PC and after the PT. Thus, the majority of the horizontal curves have full superelevation. Figure 5.3 shows one case of a superelevation profile measurement with a smartphone. The design superelevation is 4% while the measured superelevation is 4.2%. Statistical analysis showed that the average of superelevation between the 15th and 90th percentile of the length of curve is consistent with the design superelevation from the SDDOT roadway inventory.

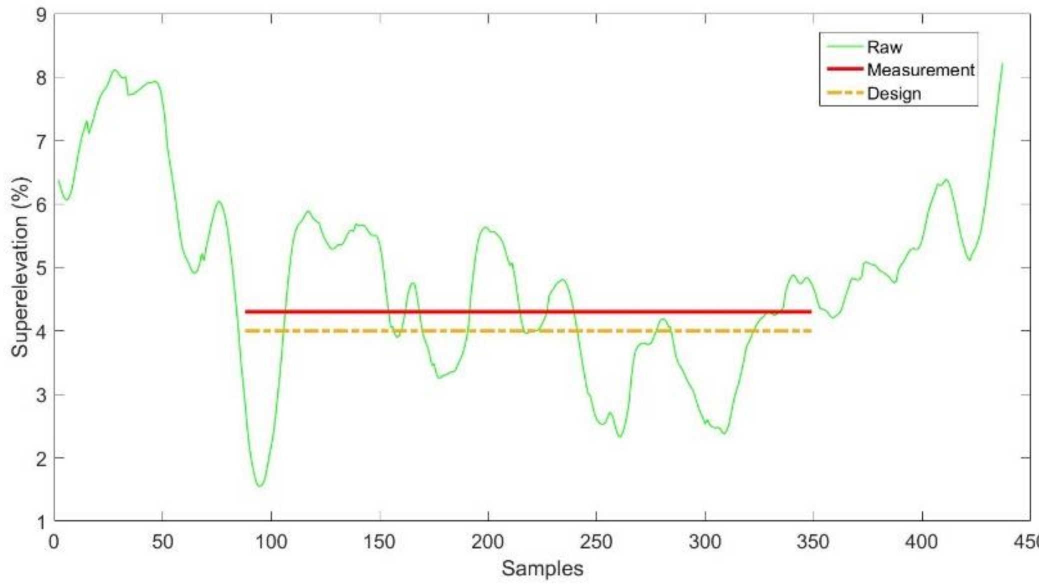


**Figure 5.3 Comparison of Design Superelevation and Measured Superelevation**

Table 3 shows the superelevation measurements for the 21 curves. In three runs, the average difference between design superelevation and measured superelevation is 1.32%, 1.56% and 1.59%, respectively. The overall superelevation difference is 0.66%. It should be noted that the comparison is between the smartphone measured superelevation and design superelevation(which may be slightly different that the as-built superelevation). However, as-built superelevation information was not available.

**Table 3 Superelevation Evaluation**

| No | Design e(%) | Survey 1 Radius | e1 | Error | Survey 2 Radius | e2 | Error | Survey 3 Radius | e3 | Error | Mean Avg | Error |
|---|---|---|---|---|---|---|---|---|---|---|---|---|
| 1 | 5.8 | 1173 | 4.0 | 1.8 | 1008 | 7.3 | -1.5 | 1033 | 5.7 | 0.1 | 5.7 | 0.1 |
| 2 | 5.8 | 1177 | 6.8 | -1.0 | 1159 | 6.2 | -0.4 | 1196 | 4.1 | 1.7 | 5.7 | 0.1 |
| 3 | 4.6 | 3594 | 3.8 | 0.8 | 3683 | 3.0 | 1.6 | 3589 | 5.5 | -0.9 | 4.1 | 0.5 |
| 4 | 5.6 | 2078 | 3.6 | 2.0 | 2056 | 3.2 | 2.4 | 2089 | 7.1 | -1.5 | 4.6 | 1.0 |
| 5 | 6 | 2290 | 6.8 | -0.8 | 2300 | 7.1 | -1.1 | 2297 | 3.9 | 2.1 | 5.9 | 0.1 |

| | | | | | | | | | | | | |
|---|---|---|---|---|---|---|---|---|---|---|---|---|
| 6 | 5.8 | 1906 | 3.8 | 2.0 | 1937 | 7.0 | -1.2 | 1872 | 3.2 | 2.6 | 4.7 | 1.1 |
| 7 | 4 | 461 | 4.5 | -0.5 | 535 | 5.0 | -1.0 | 538 | 5.8 | -1.8 | 5.1 | -1.1 |
| 8 | 5.8 | 2256 | 5.8 | 0.0 | 2275 | 2.9 | 2.9 | 2273 | 6.2 | -0.4 | 4.9 | 0.9 |
| 9 | 5.8 | 2288 | 3.9 | 1.9 | 2384 | 7.4 | -1.6 | 2294 | 3.7 | 2.1 | 5.0 | 0.8 |
| 10 | 6 | 2091 | 3.3 | 2.7 | 2088 | 8.5 | -2.5 | 2098 | 2.7 | 3.3 | 4.8 | 1.2 |
| 11 | 6 | 2085 | 6.8 | -0.8 | 2054 | 2.4 | 3.6 | 2013 | 7.9 | -1.9 | 5.7 | 0.3 |
| 12 | 6 | 2080 | 3.8 | 2.2 | 2029 | 8.5 | -2.5 | 1963 | 4.4 | 1.6 | 5.6 | 0.4 |
| 13 | 6 | 1970 | 7.8 | -1.8 | 1910 | 3.5 | 2.5 | 1979 | 8.0 | -2.0 | 6.4 | -0.4 |
| 14 | 5.8 | 2116 | 3.6 | 2.2 | 2148 | 8.0 | -2.2 | 2065 | 3.3 | 2.5 | 5.0 | 0.8 |
| 15 | 2.6 | 564 | 4.8 | -2.2 | 586 | 2.0 | 0.6 | 558 | 5.3 | -2.7 | 4.0 | -1.4 |
| 16 | 5.6 | 1901 | 5.0 | 0.6 | 1955 | 6.2 | -0.6 | 1882 | 5.1 | 0.5 | 5.4 | 0.2 |
| 17 | 4 | 1898 | 4.2 | -0.2 | 1953 | 3.2 | 0.8 | 1915 | 4.2 | -0.2 | 3.9 | 0.1 |
| 18 | 5.8 | 1489 | 7.0 | -1.2 | 1432 | 5.3 | 0.5 | 1487 | 7.3 | -1.5 | 6.5 | -0.7 |
| 19 | 6 | 1195 | 6.6 | -0.6 | 1240 | 7.5 | -1.5 | 1220 | 6.9 | -0.9 | 7.0 | -1.0 |
| 20 | 4 | 2935 | 1.8 | 2.2 | 2954 | 2.6 | 1.4 | 2555 | 5.2 | -1.2 | 3.2 | 0.8 |
| 21 | 4 | 2670 | 3.7 | 0.3 | 2596 | 3.7 | 0.3 | 2943 | 2.0 | 2.0 | 3.1 | 0.9 |
| **Average difference** | | | **1.32** | | | | **1.56** | | | **1.59** | | **0.66** |

## 5.3 Assessment of C-Alert

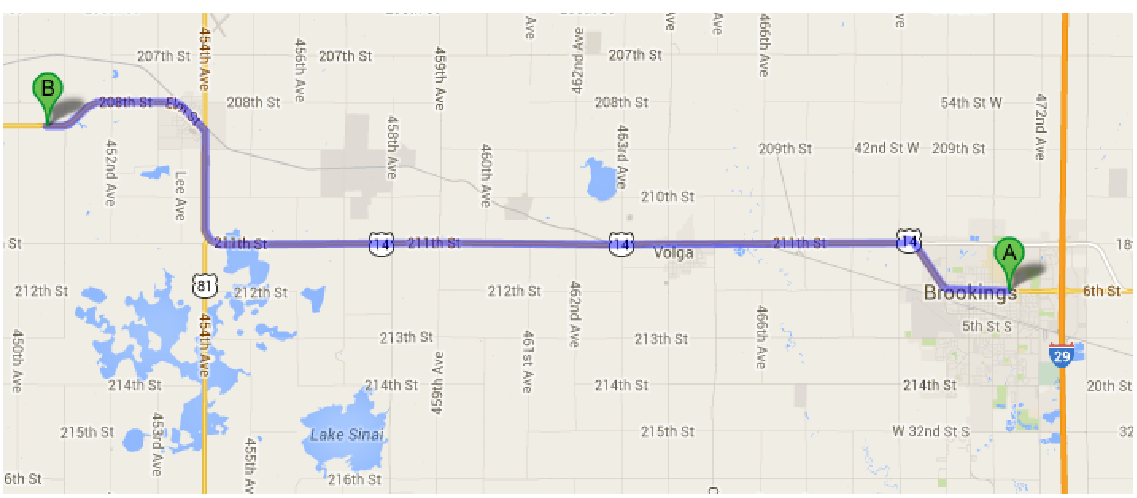


**Figure 5.4 Field Test Route of C-Alert**

Figure 5.4 shows a 30-mile test route on US Route 14 going from Brookings to Lake Preston in South Dakota used for the field test. This route has seven horizontal curves or 14 curve nodes, meaning 14 warning should be displayed during this two-way trip. Curve warning messages were recorded during two round trips. Table 4 shows that 85% of the curves were detected in the field test. Missing alerts can be attributed to a BLE connection error. The “Invalid” column refers to incorrect alerts, for example, it should be left turning warning, but it displays right turning warning. Errors can be attributed to the smartphone’s built-in GPS which dynamically searches location information and identifies the nearest curve by distance. The GPS accuracy level differs among different environments which can also result in warning errors. Hence, the GPS inaccuracy can sometimes lead to the wrong sequence of curves, particularly when two curve locations are within 500 feet from one another.

**Table 4. Assessment Result of Curve Detection Algorithm**

| Trip | Journey | Expected Alerts | Valid | Missed | Invalid |
|---|---|---|---|---|---|
| Trip 1 | $\text{Journey}_{AB}$ | 7 | 5 | 1 | 1 |
| | $\text{Journey}_{BA}$ | 7 | 6 | 0 | 1 |
| Trip 2 | $\text{Journey}_{AB}$ | 7 | 7 | 0 | 0 |
| | $\text{Journey}_{BA}$ | 7 | 6 | 0 | 1 |
| Total | | 28 | 24 | 1 | 3 |

# 6. CONCLUSIONS AND FUTURE WORK

## 6.1 Conclusions

This study included the design, implementation and evaluation of the mobile systems for low-cost real time horizontal curve inventory and warning of horizontal curves. Two smartphone applications, C-Finder and C-Alert, were developed and evaluated. The following conclusions summarize the major findings of this study:

1) Although the GPS frequency from smartphone is only 1 Hz, the field test demonstrated the proposed approach can achieve desirable radius measurement accuracy for sharp curves. The average error is approximately 3%. Since the highest accuracy of GPS is 2-5 meters, the adjusted lane width doesn't have a significant effect on the accuracy of radii estimation. However, multiple runs can achieve higher accuracy.
2) The accuracy of superelevation relies on the accuracy of curve radius, vehicle speed and acceleration rate from smartphone. Improving their accuracy can achieve more accurate superelevation measurements.
3) The work outlined in this thesis proposed a smartphone-based horizontal curve warning system using GPS, BLE technology, and HUD. In this system, a smartphone application uses a vehicle's real-time speed and position to warn drivers of imminent horizontal curves. The warning is projected on the vehicle's front windshield, therefore improving safety by not requiring drivers to look away from the road. The GPS-equipped smartphone can exchange location information in a dynamic, real-time fashion through a 3G/4G/WiFi network. Moreover, the

curve warning system uses an economically affordable device (HUD) as well as open source wireless communications that can integrate, reconfigure, and customize various data sources (e.g., state DOT data sources).

### 6.2 Future Work

Off-the-shelf smartphone technology is a potential alternative tool for horizontal curve surveys due to its low-cost and easy of application. This research focused on applying this technology to measuring simple horizontal curves. Future work should include compound, reverse, and spiral curves using smartphone sensors. The GPS frequency from smartphone is only 1 Hz. Increasing the frequency of GPS could potentially improve the radius estimation. GPS/IMU sensor fusion could be applied to increase the frequency of GPS in the future work.

C-Alert was tested via a 4G network on a selected highway route with seven curves where curve detection accuracy was evaluated. Future work should evaluate C-Alert further under various scenarios and conditions, such as BLE data transmission, GPS accuracy in different conditions (e.g., with internet and without internet, mountainous road, high density road network in urban area), and the algorithm accuracy. Human factors evaluation should also be studied to ensure that the use of this system does not introduce unintended safety issues. While C-Alert is designed for highway horizontal curves, it could also be applied to other areas such as work zones, highway-rail grade crossings, and wrong-way traffic.

## REFERENCES

[1] *Roadway Widths for Low-Traffic Volume Roads*, 1994.

[2] Traffic Safety Facts 2014.In*, No. 2015*, National Highway Traffic Safety Administration, 2015. p. 87.

[3] Li, Z., M. V. Chitturi, A. R. Bill, D. Zheng, and D. A. Noyce. Automated extraction of horizontal curve information for low-volume roads. *Transportation Research Record: Journal of the Transportation Research Board*, No. 2472, 2015, pp. 172-184.

[4] *Manual on uniform traffic control devices for streets and highways*, U.S. Department of Transpotation, 2009.

[5] Geographic Information System (GIS): Curvature Extension for ArcMap 9.x., 2010.

[6] Curve Finder FAQ for Version 2., 2010.

[7] Xu, H., and D. Wei. Improved Identification and Calculation of Horizontal Curves with Geographic Information System Road Layers. *Transportation Research Record: Journal of the Transportation Research Board*, No. 2595, 2016, pp. 50-58.

[8] Findley, D. J., C. V. Zegeer, C. A. Sundstrom, J. E. Hummer, W. Rasdorf, and T. J. Fowler. Finding and measuring horizontal curves in a large highway network: a GIS approach. *Public Works Management & Policy*, Vol. 17, No. 2, 2012, pp. 189-211.

[9] Yang, Y., and C. Zhu. Extracting road centrelines from high-resolution satellite images using active window line segment matching and improved SSDA. *International Journal of Remote Sensing*, Vol. 31, No. 9, 2010, pp. 2457-2469.

[10] Shi, W., Z. Miao, and J. Debayle. An integrated method for urban main-road centerline extraction from optical remotely sensed imagery. *IEEE Transactions on Geoscience and Remote Sensing*, Vol. 52, No. 6, 2014, pp. 3359-3372.

[11] Miao, Z., B. Wang, W. Shi, and H. Wu. A method for accurate road centerline extraction from a classified image. *IEEE Journal of Selected Topics in Applied Earth Observations and Remote Sensing,* Vol. 7, No. 12, 2014, pp. 4762-4771.

[12] Miao, Z., W. Shi, H. Zhang, and X. Wang. Road centerline extraction from high-resolution imagery based on shape features and multivariate adaptive regression splines. *IEEE geoscience and remote sensing letters,* Vol. 10, No. 3, 2013, pp. 583-587.

[13] Easa, S. M., H. Dong, and J. Li. Use of satellite imagery for establishing road horizontal alignments. *Journal of Surveying Engineering,* Vol. 133, No. 1, 2007, pp. 29-35.

[14] Dong, H., S. M. Easa, and J. Li. Approximate extraction of spiralled horizontal curves from satellite imagery. *Journal of Surveying Engineering,* Vol. 133, No. 1, 2007, pp. 36-40.

[15] Harkey, D., C. Yi, and J. Feaganes. Evaluation and validation of automated in-vehicle data collection system for developing roadway alignments. *Transportation Research Record: Journal of the Transportation Research Board*, No. 1897, 2004, pp. 164-172.

[16] Paul J. Carlson, M. B., Kit Black, and Elisabeth R. Rose. Comparison of Radius-Estimating Techniques for Horizontal Curves. *Transportation Research Record: Journal of the Transportation Research Board,Washington, D.C.,* Vol. 1918, 2005, pp. 76–83.

[17] Findley, D. J., J. E. Hummer, W. Rasdorf, and B. T. Laton. Collecting horizontal curve data: mobile asset vehicles and other techniques. *Journal of Infrastructure Systems,* Vol. 19, No. 1, 2012, pp. 74-84.

[18] Kim, J., J.-C. Lee, I.-J. Kang, S.-Y. Cha, H. Choi, and T.-G. Lee. Extraction of geometric information on highway using terrestrial laser scanning technology. *Int. Arch. Photogramm. Remote Sens. Spat. Inf. Sci,* Vol. 37, 2008, pp. 539-544.

[19] Jalayer, M., H. Zhou, J. Gong, S. Hu, and M. Grinter. A Comprehensive Assessment of Highway Inventory Data Collection Methods.In *Journal of the Transportation Research Forum, No. 53*, 2014. pp. 73-92.

[20] Uzcategui, R., and G. Acosta-Marum. Wave: A tutorial. *Communications Magazine, IEEE,* Vol. 47, No. 5, 2009, pp. 126-133.

[21] Milanes, V., J. Villagra, J. Godoy, J. Simo, J. Perez, and E. Onieva. An Intelligent V2I-Based Traffic Management System. *Intelligent Transportation Systems, IEEE Transactions on,* Vol. 13, No. 1, 2012, pp. 49-58.

[22] Zhou, Y., G. H. Evans, M. Chowdhury, K.-C. Wang, and R. Fries. Wireless Communication Alternatives for Intelligent Transportation Systems: A Case Study. *Journal of Intelligent Transportation Systems,* Vol. 15, No. 3, 2011, pp. 147-160.

[23] Maitipe, B. R., U. Ibrahim, M. Hayee, and E. Kwon. Vehicle-to-Infrastructure and Vehicle-to-Vehicle Information System in Work Zones. *Transportation Research Record: Journal of the Transportation Research Board,* Vol. 2324, No. 1, 2012, pp. 125-132.

[24] Hsu, C., C. Liang, L. Ke, and F. Huang. Verification of On-Line Vehicle Collision Avoidance Warning System using DSRC. *World Academy of Science, Engineering and Technology,* Vol. 55, 2009, pp. 377-383.

[25] Petty, K. R., and W. P. Mahoney. Enhancing road weather information through Vehicle Infrastructure Integration. *Transportation Research Record: Journal of the Transportation Research Board,* Vol. 2015, No. 1, 2007, pp. 132-140.

[26] Crabtree, J., and N. Stamatiadis. Dedicated Short-Range Communications Technology for Freeway Incident Detection: Performance Assessment Based on Traffic Simulation Data. *Transportation Research Record: Journal of the Transportation Research Board,* Vol. 2000, No. -1, 2007, pp. 59-69.

[27] Decuir, J. Introducing Bluetooth Smart: Part II: Applications and updates. *Consumer Electronics Magazine, IEEE,* Vol. 3, No. 2, 2014, pp. 25-29.

[28] Gomez, C., J. Oller, and J. Paradells. Overview and Evaluation of Bluetooth Low Energy: An Emerging Low-Power Wireless Technology. *Sensors,* Vol. 12, No. 9, 2012, pp. 11734-11753.

[29] West, A. *Smartphone, the key for Bluetooth low energy technology*. http://www.bluetooth.com/Pages/Smartphones.aspx. Accessed October 20, 2014.

[30] Donath, M., C. Shankwitz, and H. Lim. *A GPS-Based Head Up Display for Driving Under Low Visibility Conditions*. http://conservancy.umn.edu/bitstream/888/1/200303.pdf. Accessed May 20, 2014.

[31] Charissis, V., S. Papanastasiou, W. Chan, and E. Peytchev. Evolution of a full-windshield HUD designed for current VANET communication standards.In *Intelligent Transportation Systems - (ITSC), 2013 16th International IEEE Conference on*, 2013. pp. 1637-1643.

[32] Alves, P. R. J. A., J. Goncalves, R. J. F. Rossetti, E. C. Oliveira, and C. Olaverri-Monreal. Forward collision warning systems using heads-up displays: Testing usability

of two new metaphors.In *Intelligent Vehicles Symposium Workshops (IV Workshops), 2013 IEEE*, 2013. pp. 1-6.

[33] Kandhalu, A., A. E. Xhafa, and S. Hosur. Towards bounded-latency Bluetooth Low Energy for in-vehicle network cable replacement.In *Connected Vehicles and Expo (ICCVE), 2013 International Conference on*, 2013. pp. 635-640.

[34] Xia, K., X. Xu, and N. Wang. Design of vehicle control system based on bluetooth low energy smartphone platform.In *Electrical Machines and Systems (ICEMS), 2013 International Conference on*, 2013. pp. 1498-1501.

[35] Qin, X., S. Zhang, and W. Wang. Avoiding Roadway Departure Crashes with an In-Vehicle Head-Up Display.In *Transportation Research Board 94th Annual Meeting*, 2015.

[36] Aichinger, C., P. Nitsche, R. Stütz, and M. Harnisch. Using low-cost smartphone sensor data for locating crash risk spots in a road network. *Transportation Research Procedia*, Vol. 14, 2016, pp. 2015-2024.

[37] Lee, S., G. Tewolde, and J. Kwon. Design and implementation of vehicle tracking system using GPS/GSM/GPRS technology and smartphone application.In *Internet of Things (WF-IoT), 2014 IEEE World Forum on*, IEEE, 2014. pp. 353-358.

[38] Ghose, A., P. Biswas, C. Bhaumik, M. Sharma, A. Pal, and A. Jha. Road condition monitoring and alert application: Using in-vehicle smartphone as internet-connected sensor.In *Pervasive Computing and Communications Workshops (PERCOM Workshops), 2012 IEEE International Conference on*, IEEE, 2012. pp. 489-491.

[39] Raj, S., A. Jain, and R. Misra. Smartphone sensing for large data set collection of potholes.In *Proceeding of the 11th annual international conference on Mobile systems, applications, and services*, ACM, 2013. pp. 517-518.

[40] Islam, S., W. Buttlar, R. Aldunate, and W. Vavrik. Measurement of pavement roughness using android-based smartphone application. *Transportation Research Record: Journal of the Transportation Research Board*, No. 2457, 2014, pp. 30-38.

[41] Buttlar, W. G., and M. S. Islam. Integration of Smart-Phone-Based Pavement Roughness Data Collection Tool with Asset Management System.In, 2014.

[42] Zhang, S., M. Won, and S. H. Son. Low-Cost Realtime Horizontal Curve Detection Using Inertial Sensors of a Smartphone. Presented at In 84th IEEE Vehicular Technology Conference, Montréal, Canada, 2016.

[43] Manzoni, V., A. Corti, C. Spelta, and S. M. Savaresi. A driver-to-infrastructure interaction system for motorcycles based on smartphone.In *Intelligent Transportation Systems (ITSC), 2010 13th International IEEE Conference on*, 2010. pp. 1442-1447.

[44] Rodrigues, J. G. P., A. Aguiar, F. Vieira, J. Barros, and J. P. S. Cunha. A mobile sensing architecture for massive urban scanning.In *Intelligent Transportation Systems (ITSC), 2011 14th International IEEE Conference on*, 2011. pp. 1132-1137.

[45] Frank, R., W. Bronzi, G. Castignani, and T. Engel. Bluetooth Low Energy: An alternative technology for VANET applications.In *Wireless On-demand Network Systems and Services (WONS), 2014 11th Annual Conference on*, 2014. pp. 104-107.

[46] Ching-Hao, L., and Y. Chia-Chen. An Efficient Real-Time Traffic Sign Recognition System for Intelligent Vehicles with Smart Phones.In *Technologies and Applications of Artificial Intelligence (TAAI), 2010 International Conference on*, 2010. pp. 195-202.

[47] Mackensen, E., M. Lai, and T. M. Wendt. Bluetooth Low Energy (BLE) based wireless sensors.In *Sensors, 2012 IEEE*, 2012. pp. 1-4.

[48] Adafruit. *32X16 RGB LED Matrix*. https://learn.adafruit.com/32x16-32x32-rgb-led-matrix/overview. Accessed March 20, 2014.

[49] Welch, G., and G. Bishop. An introduction to the Kalman filter. 1995.

[50] Han, J., J. Pei, and M. Kamber. *Data mining: concepts and techniques*. Elsevier, 2011.

[51] AASHTO. *A Policy on Geometric Design of Highways and Streets*. 2011.

[52] Figueroa Medina, A., and A. Tarko. Speed factors on two-lane rural highways in free-flow conditions. *Transportation Research Record: Journal of the Transportation Research Board*, No. 1912, 2005, pp. 39-46.

[53] Hu, W., and E. T. Donnell. Models of acceleration and deceleration rates on a complex two-lane rural highway: Results from a nighttime driving experiment. *Transportation research part F: traffic psychology and behaviour*, Vol. 13, No. 6, 2010, pp. 397-408.

[54] Wood, J., and E. Donnell. Stopping sight distance and horizontal sight line offsets at horizontal curves. *Transportation Research Record: Journal of the Transportation Research Board*, No. 2436, 2014, pp. 43-50.